

Universidade Estadual de Campinas

Instituto de Física “Gleb Wataghin”

Tese de Doutoramento

Estudo teórico de complexos excitônicos em poços quânticos de semicondutores

Luis Carlos Ogando Dacal

Orientador: Prof. Dr. José Antonio Brum

Co-orientadora: Profa. Dra. Maria José Santos Pompeu Brasil

Tese apresentada ao Instituto de Física
“Gleb Wataghin” da Universidade
Estadual de Campinas como requisito para
obtenção do título de Doutor em Física.

Campinas, 29 de agosto de 2001

A meu pai, sempre presente
mesmo depois da partida.

“O que sacia a alma não é o muito saber,
mas o saborear as coisas internamente.”
(Santo Inácio de Loyola)

Agradecimentos

- A Deus por não desistir de mim.
- À minha família, minha mãe, Pila, Leo e Manise por me apoiarem sempre e em tudo.
- À ❤️Luluzinha❤️ por me amar e me ensinar a amar.
- Ao Prof. José Brum pela amizade, paciência e dedicação.
- À Profa. Maria José pela orientação na “parte experimental” do meu doutoramento.
- Aos doutores Gerald Bastard e Robson Ferreira por me receberem e me orientarem durante o estágio na França.
- Aos professores do GPO : Eliermes, Cerdeira, Fernando e Peter pela paciência e pelas inúmeras contribuições à minha formação.
- À Lene e ao Milton pela dedicação, carinho e pelo lanche.
- Aos meus “padrinhos-afilhados” : Serginho e Silvinha pela amizade a toda prova.
- Aos colegas do GPO : Alexandre, Ana, Carol, Daniel, Edson Laureto, Edson Ribeiro, Gustavo, Helô, Hugo, Ivan, Javier, Jorge, Luciana, Marcelo, Marcio, Marcos, Michel, Odilon, Rodrigo pelo bom humor, risadas e companheirismo.
- À turma da sala de alunos do DFMC : Caetano (e Patricinha), Liliana e alunos do GPO que sempre andavam por lá.
- Aos colegas de casa : Almir, Kely, Di, Ricardo e Juliana por suportarem meu mau humor.
- Aos amigos e amigas que fizeram e farão sempre parte da minha vida (Nilda, Alysson, Maria Elena e Célio, Andres e Flavinha, Germano, Daniel, Chico, Felipe, Pe. Toninho, Pe. Ramon, Denis e Bete, ...)
- Ao CNPq e à FAPESP pelo suporte financeiro.

Índice

Resumo.....	1
Abstract.....	2
Capítulo 1.....	3
Introdução geral e motivação.....	4
1) Poços quânticos.....	4
2) Vantagens dos materiais semicondutores.....	5
3) Breve histórico.....	6
4) Modelos e aproximações utilizados.....	7
5) Apresentação dos capítulos seguintes.....	9
6) Bibliografia.....	9
Capítulo 2.....	11
Charged excitons binding energy in semiconductor quantum wells in the presence of longitudinal electric fields.....	12
1) Introduction.....	13
2) Model.....	15
A) Exciton Hamiltonian.....	17
B) Charged exciton Hamiltonian.....	18
3) Results and discussions.....	19
4) Conclusion.....	25
5) Acknowledgements.....	26
References.....	26
Capítulo 3.....	28
Excitons carregados na presença de campos magnéticos longitudinais.....	29
1) Introdução.....	29
2) Éxciton com campo magnético.....	30
3) X ⁻ com campo magnético.....	32
4) Resultados e discussões.....	34

5) Conclusões.....	41
6) Bibliografia.....	41
Capítulo 4.....	42
The interface defect influence on the ionization energy of charged excitons in semiconductor quantum wells..... 43	
1) Introduction.....	44
2) Model.....	45
A) Exciton Hamiltonian.....	47
B) Charged exciton Hamiltonian.....	49
3) Results and discussions.....	50
4) Conclusion.....	54
5) Acknowledgements.....	55
References.....	55
Capítulo 5.....	57
Negatively charged donors in semiconductor quantum wells in the presence of longitudinal magnetic and electric fields..... 58	
1) Introduction.....	59
2) Model.....	61
A) Neutral donor Hamiltonian.....	63
B) Negatively charged donor Hamiltonian.....	63
3) Results and discussions.....	64
4) Conclusion.....	72
5) Acknowledgements.....	72
References.....	73
Capítulo 6.....	74
Conclusão geral.....	75

Resumo

Um sistema físico com presença de partículas indistinguíveis interagentes cria a rica possibilidade do estudo dos efeitos de correlação e troca, os quais são frutos desta indistinguibilidade. O complexo mais simples para a manifestação destes efeitos seria aquele onde apenas duas partículas indistinguíveis estão presentes. Em física da matéria condensada, estes complexos são os excitons, os doadores e os aceitadores carregados. No caso específico de poços quânticos semicondutores, a não parabolicidade da banda de valência faz com que excitons e doadores negativamente carregados sejam os complexos com modelamento teórico mais simples.

Apesar da previsão da estabilidade dos excitons carregados (“trions”) ter sido feita no final da década de 50 para os materiais semicondutores tipo “bulk”, sua primeira observação experimental só ocorre no início da década de 90 e em poços quânticos, onde o confinamento unidimensional das cargas aumenta a energia de ligação destes complexos em uma ordem de grandeza. Desde então iniciou-se uma intensa pesquisa a respeito da física destes complexos pois a blindagem das interações coulombianas nos materiais semicondutores permite que campos magnéticos usuais em laboratórios sejam capazes de provocar fortes alterações na energia de ligação dos “trions”. Outra rica possibilidade de investigação é o fato dos excitons carregados aparecerem como um estado intermediário entre o exciton neutro e a singularidade do nível de Fermi quando a concentração de elétrons dopantes na amostra é aumentada.

Nesta tese apresentamos um estudo teórico dos excitons carregados e dos doadores negativamente carregados em poços quânticos de $\text{GaAs}/\text{Al}_{0.3}\text{Ga}_{0.7}\text{As}$ considerando os efeitos da presença de campos elétricos e magnéticos externos. Nossa contribuição acrescenta um método simples, preciso e fisicamente transparente para o modelamento teórico destes complexos em contraposição às poucas e complexas abordagens até agora apresentadas na literatura científica. Nossos resultados mostram que os defeitos de interface dos poços quânticos desempenham um papel fundamental na dinâmica dos “trions” contrariando as conclusões de alguns estudos experimentais, mas confirmando a visão de outros.

Abstract

A physical system where indistinguishable particles interact with each other creates the possibility of studying correlation and exchange effects. The simplest system is that one with only two indistinguishable particles. In condensed matter physics, these complexes are represented by charged excitons, donors and acceptors. In quantum wells, the valence band is not parabolic, therefore, the negatively charged excitons and donors are theoretically described in a simpler way.

Despite the fact that the stability of charged excitons (trions) is known since the late 50s, the first experimental observation occurred only at the early 90s in quantum well samples, where their binding energies are one order of magnitude larger due to the one dimensional carriers confinement. After this, these complexes became the subject of an intense research because the intrinsic screening of electrical interactions in semiconductor materials allows that magnetic fields that are usual in laboratories have strong effects on the trion binding energy. Another rich possibility is the study of trions as an intermediate state between the neutral exciton and the Fermi edge singularity when the excess of doping carriers is increased.

In this thesis, we present a theoretical study of charged excitons and negatively charged donors in $\text{GaAs}\backslash\text{Al}_{0.3}\text{Ga}_{0.7}\text{As}$ quantum wells considering the effects of external electric and magnetic fields. We use a simple, accurate and physically clear method to describe these systems in contrast with the few and complex treatments available in the literature. Our results show that the QW interface defects have an important role in the trion dynamics. This is in agreement with some experimental works, but it disagrees with other ones.

Capítulo 1

Introdução geral e motivação

1) POÇOS QUÂNTICOS

Quando um material semicondutor é crescido entre duas camadas de um material de “gap” maior, forma-se um poço de potencial (poço quântico) que é responsável pelo confinamento de portadores livres na direção de crescimento desta estrutura. Para larguras de poço da ordem do raio de Bohr efetivo, estes sistemas de baixa dimensionalidade (quase 2D) apresentam efeitos quânticos discretizando a dinâmica dos portadores na direção do confinamento.

Considerando materiais intrínsecos (sem dopagem), a excitação óptica destas estruturas cria elétrons na banda de condução deixando um número equivalente de buracos na banda de valência. O espectro óptico obtido é dominado pela interação coulombiana entre as cargas fotogeradas. Experimentalmente, observa-se a luminescência de um complexo formado pela atração entre um elétron e um buraco. Este par de cargas interagentes recebe o nome de exciton sendo o análogo do átomo de hidrogênio (H) na física de semicondutores.

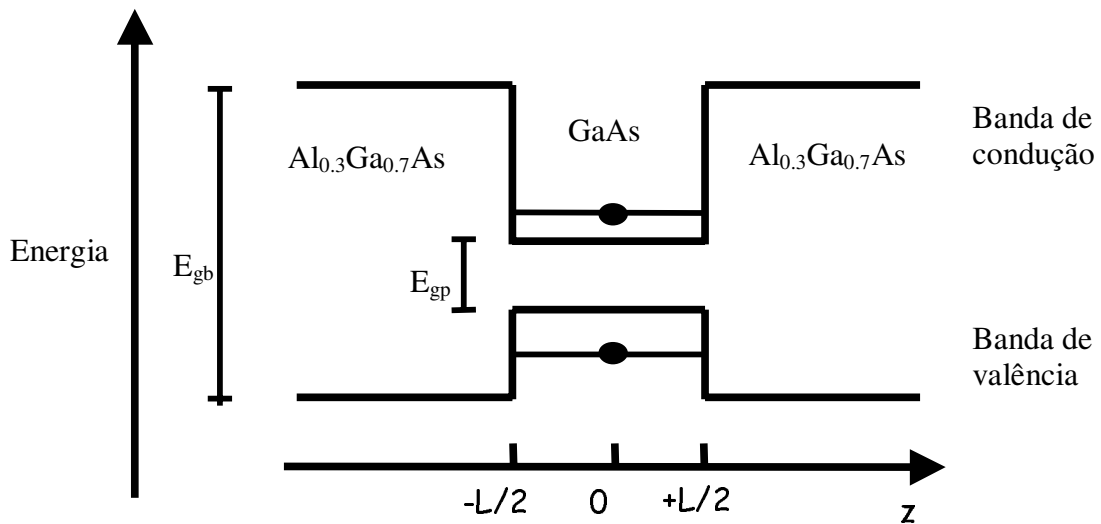


Figura 1 – Dispersão de energia na direção de crescimento (z) de poço quântico de semicondutor. Níveis fundamentais do poço de potencial e par elétron-buraco(exciton) estão representados.

Quando uma dopagem modulada é introduzida na barreira de potencial, portadores adicionais, elétrons no caso de dopagem com doadores ou buracos no caso de dopagem com aceitadores, tunelam da barreira para o poço ficando confinados neste último. Cria-se, então, a possibilidade do estudo do efeito da presença deste excesso de portadores no espectro óptico destas estruturas. A interação coulombiana entre um elétron (buraco) extra e o dipolo elétrico de um exciton opticamente criado forma um complexo carregado chamado X^- (X^+) ou de forma mais genérica “trion”. Este complexo é por sua vez o análogo do íon H^- (H_2^+) em física de semicondutores. O “trion” é portanto um dos complexos mais simples para o estudo dos efeitos de correlação e troca em sistemas de “muitos” corpos.

Nesta tese, apresentaremos um estudo teórico de complexos excitônicos em poços quânticos de semicondutor. Consideraremos, mais especificamente, poços quânticos de GaAs entre barreiras de $Al_{0.3}Ga_{0.7}As$ (figura 1). Serão considerados os efeitos da presença de campos elétricos e magnéticos paralelos à direção de crescimento (longitudinais) e de defeitos estruturais na interface entre poço e barreira. Também analisaremos o D^- , um complexo análogo ao X^- , mas com a carga positiva (centro atrativo) fixa.

2) VANTAGENS DOS MATERIAIS SEMICONDUTORES

O estudo dos “trions” em materiais semicondutores apresenta uma importante vantagem sobre o estudo do H^- (ou H_2^+) em física atômica. A blindagem das interações coulombianas no semicondutor permite que campos magnéticos alcançáveis em laboratório consigam gerar energias ciclotrônicas comparáveis à energia coulombiana. Considerando-se o exciton em estruturas semicondutoras de GaAs massivo (tipo “bulk”), isto é atingido para campos magnéticos da ordem de 3 T. No caso do átomo H, precisa-se de campos da ordem de 10^5 T. Tais campos somente são observados em sistemas estelares como, por exemplo, anãs brancas e estrelas de neutrons. Desta forma, em laboratório, pode-se alterar fortemente a energia de ligação do “trion” e passar de um regime onde o campo magnético é uma perturbação para um regime onde ele domina as interações.

Outra vantagem é que a interação entre o excesso de cargas dopante confinado no poço e o “trion” possibilita a investigação de efeitos de muitos corpos através do controle da densidade de portadores dopantes. Isto permite o estudo da evolução do pico de absorção do exciton para o pico da singularidade do nível de Fermi passando pelo do “trion” [1].

3) BREVE HISTÓRICO

A seguir, apresentaremos um resumo que de maneira geral mostra a evolução e o estado atual da pesquisa sobre “trions”.

O primeiro trabalho a mostrar a estabilidade dos excitons carregados em semicondutores tipo “bulk” foi de Lampert [2] já em 1958. No entanto, os valores da energia de ligação são muito pequenos para serem experimentalmente verificados. Em 1974, Munsch y Stébé [3] mostraram que este valor é aumentado em uma ordem de grandeza quando há confinamento de cargas em uma direção, ou seja, em amostras de poços quânticos. Apesar disto, a energia de ligação obtida era da ordem de poucos meV exigindo amostras de alta qualidade que permitissem resolver os picos de luminescência para o exciton e para o “trion”.

A primeira verificação experimental de um “trion” só ocorreu em 1993. Kheng *et al.* [4] fizeram esta verificação em poços quânticos de materiais II-VI onde a energia de ligação do “trion” é mais que o dobro da verificada nos III-V. A presença dos “trions” em poços de GaAs é mostrada pouco tempo depois [5,6].

A partir destes trabalhos, teve início uma intensa pesquisa sobre “trions”. Chama especial atenção a presença de trabalhos experimentais com resultados que indicam tendências opostas sobre o caráter livre ou localizado dos portadores que formam o exciton carregado. Alguns autores afirmam que estas cargas são localizadas pelas flutuações dos potenciais dos dopantes ionizados [7,8]. Outros atribuem a discrepância entre resultados experimentais e teóricos a existência de defeitos estruturais na interface do poço [9]. Apesar disto, existem trabalhos que indicam que as cargas estão livres no plano perpendicular à direção de crescimento através da análise do tempo de vida destes portadores [10,11].

Riva *et al.* calculam a energia de ligação do X⁻ na ausência [9] e na presença [12] de campos magnéticos longitudinais. Eles utilizam o *método variacional estocástico* com uma base de *funções gaussianas correlacionadas deformadas* obtendo uma boa concordância com os resultados experimentais. Whittaker e Shields [13] usam uma base de níveis de Landau para descrever a dinâmica do X⁻ no plano perpendicular ao poço e mostram a importância da inclusão de mais de um nível de poço para a descrição do X⁻ no limite de altos campos magnéticos (limite de validade dos cálculos). Por fim, o trabalho de Dzyubenko e Sivachenko [14] mostra que a resposta óptica do estado fundamental tipo tripleno só é possível quando há quebra de simetria no poço.

Nosso trabalho tem por objetivo contribuir no esclarecimento das dúvidas citadas anteriormente e possibilitar um melhor modelamento teórico dos complexos excitônicos em poços quânticos de semicondutor. O método que utilizamos enfatiza a intuição física e possui grande flexibilidade, permitindo sua aplicação em diferentes situações.

4) MODELOS E APROXIMAÇÕES UTILIZADAS

O modelo de massa efetiva foi empregado para descrever os materiais semicondutores e o de função envelope para descrever a heteroestrutura (poço quântico). Eles já foram largamente empregados na descrição de poços de GaAs com barreiras de AlGaAs, nos garantindo a segurança necessária para o desenvolvimento de nossa pesquisa [15].

Materiais semicondutores tipo III-V “bulk” possuem dispersões de energia parabólicas. Em um poço quântico, esta dispersão é alterada no plano perpendicular ao poço sendo que a banda de valência é mais fortemente afetada. A quebra da simetria de translação na direção de crescimento remove a degenerescência das bandas de buraco leve e pesado na região de $\vec{k} = 0$. A figura 2 mostra esta dispersão não parabólica da banda de valência para poços de GaAs de 100 Å e 150 Å. Podemos perceber também que a aproximação parabólica para estas dispersões é razoável, principalmente para a primeira banda de buraco pesado (HH₁) nas proximidades de $\vec{k} = 0$. Nossa trabalho assumiu

dispersões parabólicas para elétrons e buracos pesados (HH_1), o que é mais crítico no caso do X^+ .

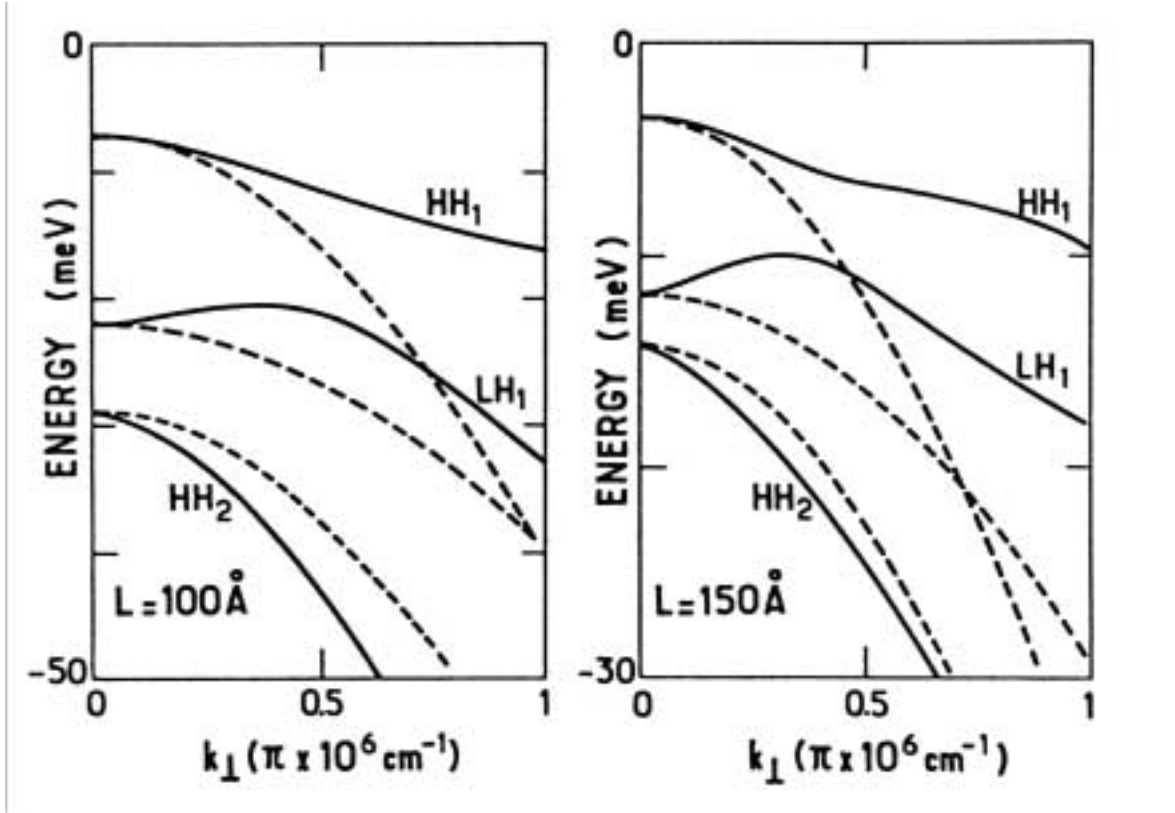


Figura 2 – Dispersão da banda de valência no plano perpendicular à direção de crescimento do poço quântico de $GaAs/Al_{0.3}Ga_{0.7}As$ para larguras de 100 e 150 Å. As linhas tracejadas correspondem às respectivas aproximações parabólicas [15].

Os efeitos da interação do gás de portadores dopantes com o “trion”, ou seja, blindagem e preenchimento do espaço de fase foram ignorados. Vale ressaltar que a inclusão destes efeitos tende a reduzir a energia de ligação do “trion”. De maneira geral, para uma densidade de portadores da ordem de $10^{11}.cm^{-2}$, o exciton negativamente carregado não é mais um estado ligado [1]. Estes resultados são confirmados teoricamente através de um cálculo incluindo a blindagem na aproximação RPA (“random phase approximation”) e levando em conta o princípio de exclusão de Pauli [16].

Consideramos ainda valores idênticos para os parâmetros efetivos (massas efetivas e constante dielétrica) dos materiais do poço e das barreiras, ou seja, os efeitos de *carga*

imagem foram desprezados. Nossos resultados devem ser vistos, portanto, como um limite superior para o valor da energia de ligação.

5) APRESENTAÇÃO DOS CAPÍTULOS SEGUINTE

O capítulo 2 apresenta os resultados dos nossos cálculos para a energia de ligação de “trions” em função da largura do poço quântico e o efeito da presença de um campo elétrico longitudinal. Ele corresponde a um artigo submetido à “Physical Review B” e é apresentado em formato aceito pela referida revista.

O capítulo 3 trata da inclusão de um campo magnético longitudinal no Hamiltoniano dos excitons carregados e o seu efeito na energia de ligação destes.

O capítulo 4 apresenta os primeiros resultados para a energia de ligação de “trions” levando-se em consideração a presença de defeitos estruturais na interface entre poço e barreira. Este capítulo e o de número 5 também correspondem a artigos submetidos à “Physical Review B”.

O capítulo 5 apresenta os resultados obtidos para a energia de ligação de doadores negativamente carregados com o centro atrativo localizado no interior do poço quântico. Neste capítulo são considerados os efeitos da presença de campos elétricos e magnéticos longitudinais sobre a energia de ligação destes complexos assim como a influência da posição do centro atrativo. O doador negativamente carregado é um problema que foi incluído como um caso limite do “trion” quando a massa de buraco tende a infinito, ou seja, é fixa.

O capítulo 6 mostra as conclusões gerais do nosso trabalho.

6) BIBLIOGRAFIA

- [1] V. Huard, R. T. Cox, K. Saminadayar, A. Arnoult and S. Tatarenko, Phys. Rev. Lett. **84**, 187 (2000).
- [2] M. A. Lampert, Phys. Rev. Lett. **1**, 450 (1958).

- [3] G. Munsch and B. Stébé, Phys. Status Solidi (b) **64**, 213 (1974).
- [4] K. Kheng, R. T. Cox, Y. Merle d'Aubigné, Franck Bassani, K. Saminadayar and S. Tatarenko, Phys. Rev. Lett. **71**, 1752 (1993).
- [5] A. J. Shields, J. L. Osborne, M. Y. Simmors, M. Pepper and D. A. Ritchie, Phys. Rev. B **52**, R5523 (1995).
- [6] G. Finkelstein, H. Shtrikman, I. Bar-Joseph, Phys. Rev. B **53**, R1709 (1996).
- [7] G. Eytan, Y. Yayon, M. Rappaport, H. Shtrikman and I. Bar-Joseph, Phys. Rev. Lett. **81**, 1666 (1998).
- [8] D. Brinkmann, J. Kudrna, P. Gilliot, B. Hönerlage, A. Arnoult, J. Cibert and S. Tatarenko, Phys. Rev. B **60**, 4474 (1999).
- [9] C. Riva, F. M. Peeters and K. Varga, Phys. Rev. B **61**, 13873 (2000).
- [10] Arza Ron, H. W. Yoon, M. D. Sturge, A. Manassen, E. Cohen and L. N. Pfeiffer, Solid State Commun. **97**, 741 (1996) .
- [11] V. Ciulin, P. Kossacki, S. Haacke, J.-D. Ganière, B. Deveaud, A. Esser, M. Kutrowski and T. Wojtowicz, Phys. Rev. B **62**, R16310 (2000).
- [12] C. Riva, F. M. Peeters and K. Varga, Phys. Rev. B **63**, 115302-1 (2001).
- [13] D. M. Whittaker and A. J. Shields, Phys. Rev. B **56**, 15185 (1997).
- [14] A. B. Dzyubenko and A. Yu. Sivachenko, Phys. Rev. Lett. **84**, 4429 (2000).
- [15] G. Bastard, *Wave Mechanics Applied to Semiconductro Heterostructures* (Les Éditions de Physique, 1988).
- [16] L. C. O. Dacal and J. A. Brum, not published.

Capítulo 2

Charged excitons binding energy in semiconductor quantum wells in the presence of longitudinal electric fields

Luis C. O. Dacal¹, José A. Brum^{1,2}

(1) *IFGW-DFMC, Universidade Estadual de Campinas,*

C.P. 6165, 13083-970, Campinas-SP, Brazil and

(2) *Laboratório Nacional de Luz Síncrotron - ABTLuS,*

C. P. 6192, 13084-971, Campinas-SP, Brazil

Abstract

We present variational calculations of the binding energy for positively and negatively charged excitons (trions) in idealized GaAs/Al_{0.3}Ga_{0.7}As quantum wells with parabolic electrons and holes energy dispersions. The configuration interaction method is used with a physically meaningful single-particle basis set. We have shown that the inclusion of more than one electron quantum well solution in the basis is important to obtain accurate values for the binding energies. The effects of longitudinal electric field and quantum well confinement on the charged excitons bound states are studied and the conditions for the trion ionization are discussed.

I. INTRODUCTION

A quantum well (QW) is a layer of low energy gap material grown between two others with larger gaps. This energy difference gives rise to electron and hole confinement in the lower gap material for type I QWs. In this type of semiconductor heterostructures, the optical transitions are dominated by Coulomb interactions.

In intrinsic QWs under low excitation power, when the same amounts of electrons and holes are present, the complex that dominates the photoluminescence spectrum is a neutral complex, the exciton, formed by the Coulomb interaction between one electron and one hole. On the other hand, in the case of a lightly modulation doped QW, the charge excess makes possible that the excitonic electrical dipole binds an extra carrier forming a charged complex (trion). In the case of a p-doped QW, the positive complex may be a bound state (X^+). It is analogous to the H_2^+ molecule in atomic physics. On the other hand, the negative complex (X^-) may be detected in n-doped structures and it is analogous to H^- . The stability of such charged complexes in semiconductors was first proposed by Lampert [1].

An interesting aspect of these complexes in semiconductor materials is that magnetic fields available in laboratories produce strong effects on their binding energies. This creates a rich experimental situation that would only be possible in astrophysical systems for the cases of H^- and H_2^+ . Unfortunately, the calculated trion binding energy for semiconductor bulk materials [2] showed that its value is too low to be experimentally detected. However, this value is one order of magnitude larger in semiconductor quantum wells [3] as a consequence of the carriers confinement. This opened new experimental possibilities in the case of high-quality samples.

The first experimental observation of a trion spectrum was made by Kheng *et al.* [4] in a II-VI QW. In this case the trion binding energy is more than twice the value for III-V systems [5]. Glasberg *et al.* [6] investigated X^+ and X^- in the same sample and they showed that the binding energy of the negative trion singlet state increases faster than the positive one as a function of the magnetic field.

The X^- has been theoretically studied in the presence [7–9] and in the absence [10] of longitudinal magnetic field (applied along the growth direction) through different techniques. The *stochastic variational method* with a basis set of *deformed correlated gaussian functions* was used by Riva *et al.* [8] and a good agreement with experiments was obtained. Whittaker and Shields [9] worked with a Landau levels basis set for the in-plane (xy) motion and showed the importance of including more than one QW level in the z (growth) direction wavefunction component. In this case, the quasi-2D nature of the problem was explored, which was enhanced by the magnetic field applied parallel to the growth direction.

The X^- theoretical treatment is difficult. It is a few-body problem and, in our case, the low dimensionality has to be added to its complexity. Although the trion is a ground-state, making it suitable for variational techniques, its stability can only be determined in comparison with its first excited state. Generally, this is an excitonic state with a noninteracting extra electron (X^-) which is also variationally determined. As a consequence, it is rather complicated to determine the accuracy of the calculated trion binding energy.

The previous works did not succeed in presenting a detailed analysis of the exchange and correlation effects on the trion electronic structure. How the presence of the extra carrier affects the excitonic orbitals is an unclear question. To shed some light to this problem, we use the configuration interaction method [11] to build up a **physically clear** basis set and to calculate variational binding energies of positively and negatively charged excitons in idealized GaAs/Al_{0.3}Ga_{0.7}As quantum wells. We study the effects of the quantum well confinement and longitudinal electric field on the charged exciton bound states. Our basis allows us to have a good idea on the different contributions of the trion degrees of freedom to its binding energy.

II. MODEL

We consider a semiconductor QW, more exactly a GaAs layer between two Al_{0.3}Ga_{0.7}As layers treated within the effective mass and envelope function frameworks considering the z as the growth direction. The position z = 0 is the quantum well center and we neglect the band bending due to the doping. This means that the electron and hole QW wavefunctions have well defined parities. We also consider ideal QW interfaces, neglecting interdiffusion and doping potential fluctuations effects. The valence and conduction subbands are approximated by parabolic dispersions what is less accurate for holes. Therefore, this approximation is more severe in the case of X⁺.

We start with the assumption that the QW confinement is strong enough to make a z and (x,y) separable wavefunction in the basis set reasonable. We use the noninteracting electron and hole QW solutions as the z-part of the one particle trial wavefunctions. When a longitudinal electric field (z axis) is present, the QW solutions are given by Airy functions [12], which do not have well defined parities. The continuum of states is emulated by a finite set of discrete states generated by a larger QW (1000 Å) with infinite barriers embedding the structure we are interested in.

The axial symmetry leads us to use polar coordinates to describe the X⁻ in-plane motion in terms of center of mass (CM) and relative to the hole coordinates :

$$\begin{aligned}\vec{\rho}_1 &= \vec{\rho}_{e1} - \vec{\rho}_h \\ \vec{\rho}_2 &= \vec{\rho}_{e2} - \vec{\rho}_h \\ \vec{\rho}_{CM} &= \frac{m_e(\vec{\rho}_{e1} + \vec{\rho}_{e2}) + m_{hxy}\vec{\rho}_h}{m_{hxy} + 2m_e},\end{aligned}\tag{1}$$

where the electron mass is isotropic. On the other hand, the hole dispersion is strongly non-parabolic in QWs, but, as a first approximation, the off-diagonal terms of the Luttinger Hamiltonian can be neglected. In this case, the hole mass is anisotropic and shows a lighter in-plane value. The CM mass is given by m_{hxy}+2m_e. We use the same mass values for the well and the barrier materials. In this approximation, the X⁺ in-plane

coordinates are easily obtained from the previous ones through the electron and hole labels interchange.

We label the trion states through the quantum numbers associated with the constants of motion, namely, the CM wave-vector (K_{CM}), the z component of the total angular momentum ($M=m_1+m_2$) and the total spin ($S=S_1+S_2$).

The CM motion is uncoupled to the internal dynamics and it is described by a plane wave. Consequently, it will not be explicitly considered here. However, it is important to notice that in the presence of a magnetic field, the CM and internal degrees of freedom are coupled since the trion is a charged complex.

The two electrons in X^- (holes in the case of X^+) are indistinguishable and the configuration interaction method is used to build up a non-orthogonal two-particle basis, in other words, we work with a basis set of Slater determinants and solve the *generalized eigenvalue problem*.

The spatial part of the charged exciton trial wavefunction with total relative particle angular momentum equal to M is given by :

$$\Psi_{(m+n=M)} = \sum_{i,j,m,n,p,q,r} c_{i,j,m,n,p,q,r} N_{i,j,m,n,p,q,r} \chi_p(z_h) \\ \times \left[\chi_q(z_{e1}) \phi_i^m(\vec{\rho}_1) \chi_r(z_{e2}) \phi_j^n(\vec{\rho}_2) \pm \chi_r(z_{e1}) \phi_j^n(\vec{\rho}_1) \chi_q(z_{e2}) \phi_i^m(\vec{\rho}_2) \right], \quad (2)$$

where $c_{i,j,m,n,p,q,r}$ is a linear variational parameter, $N_{i,j,m,n,p,q,r}$ is the determinant normalization, $\chi_q(z)$ is the q th electron (e) or hole (h) QW solution, $\phi_i^m(\vec{\rho})$ is one relative particle wavefunction. The sum over the integer numbers m and n is restricted by the total relative particle angular momentum conservation : $M=m+n$. In equation (2) “+” builds up the singlet states while “-” builds up the triplet ones. In the absence of magnetic field, only the singlet ($M=0$) is a bound state.

The in-plane relative particle wavefunction is given by :

$$\phi_j^m(\vec{\rho}) = N_{j,m} \rho^m \exp \left[-\frac{\rho^2}{\lambda_j^2} \right] \exp [im\theta] \quad (3)$$

where $N_{j,m}$ is the relative particle function normalization, λ_j is an element of a set of physically meaningful parameters that determines the basis size and m is an integer that defines the relative particle angular momentum. There is one set of λ parameters for each angular momentum. They are chosen through a geometric progression [13].

The main advantages of the trial wavefunction, Eq. (2), rely on its analytical integration and its physical transparency. The relative particles are composed by one positive and one negative charge, therefore we work with in-plane one particle functions that have the symmetry of two-dimensional atomic orbitals.

Analogously to the charged exciton case, the trial wavefunction of the neutral complex, the exciton, is given by :

$$\psi_m = \sum_{i,j,k} c_{i,j,k} N_{i,j,k} \chi_i(z_h) \chi_j(z_e) \phi_k^m(\vec{\rho}) \quad (4)$$

where $\vec{\rho} = \vec{\rho}_e - \vec{\rho}_h$.

In the following, we analyze the two different exciton complexes.

A. Exciton Hamiltonian

The exciton CM is a free particle, so we can omit its energy contribution. Using the relative coordinate for the in-plane motion, the exciton Hamiltonian is written as :

$$H_{ex} = H(z_e) + H(z_h) + T_{xy} + V_c, \quad (5)$$

where

$$H(z_{e,h}) = -\frac{\hbar^2}{2m_{e,hz}} \frac{\partial^2}{\partial z_{e,h}^2} + V_{we,wh} Y\left(\frac{L}{2} - |z_{e,h}|\right), \quad (6)$$

$$T_{xy} = -\frac{\hbar^2}{2\mu} \left[\frac{1}{\rho} \frac{\partial}{\partial \rho} \left(\rho \frac{\partial}{\partial \rho} \right) + \frac{1}{\rho^2} \frac{\partial^2}{\partial \theta^2} \right], \quad (7)$$

$$V_c = -\frac{e^2}{\varepsilon \sqrt{(z_e - z_h)^2 + \rho^2}}. \quad (8)$$

Here the QW potential height for electrons (e) and holes (h) is given by $V_{we,wh}$, $Y(z)$ is the step function ($Y(z)=1$ if $z>0$ and $Y(z)=0$ if $z<0$), L is the QW width, μ is the exciton reduced mass and $\varepsilon=13.2$ is the GaAs dielectric constant.

The relative particle angular momentum conservation assumes a simple form in the exciton case. The in-plane part of Eq. (5) is an effective one particle Hamiltonian and the exciton ground state basis set is built up with s-like functions. This means that m is a good quantum number and only $m=0$ terms have to be taken into account in Eq. (4).

We obtain good convergence for the exciton ground state binding energy with 7 lambda factors between 5 and 800 Å. The coupling of different conduction and valence QW subbands gives only marginal contributions to the energy [14]. Despite of this, we used a basis set with 3 (2) QW levels for electrons (holes) since they are necessary in the charged exciton case. The full basis set has 42 states.

B. Charged exciton Hamiltonian

Analogously to the exciton case, using the relative to the hole coordinates for the in-plane motion (Eq. (1)), the X^- Hamiltonian is given by :

$$H_{ce} = H_{ex}(1) + H_{ex}(2) - \frac{\hbar^2}{m_{hxy}} \vec{p}_1 \cdot \vec{p}_2 + \frac{e^2}{\varepsilon} \frac{1}{\sqrt{|\vec{\rho}_1 - \vec{\rho}_2|^2 + (z_{e1} - z_{e2})^2}} \quad (9)$$

where \vec{p}_i is the in-plane linear momentum operator corresponding to the i th relative particle. The term proportional to $\vec{p}_1 \cdot \vec{p}_2$ is a consequence of our choice of coordinates transformation (Eq. (1)). This term is inversely proportional to the hole mass and it represents the hole mobility [15].

The X^+ parabolic Hamiltonian is immediately obtained from Eq. (9) through the interchange of the electron and hole labels.

The charged exciton binding energy (E_b) is defined as the difference between the energy of this charged complex and the energy of an exciton (X^0) plus an in-plane free electron, in the X^- case, or a free hole, in the X^+ case. Taking the ground state energy of these carriers as zero, one can write :

$$E_b(X^-/X^+) = E(X^-/X^+) - E(X^0) \quad (10)$$

It is important to emphasize that the charged exciton binding energy is a difference between two values obtained variationally. This means that the calculated trion binding energy is not necessarily an upper limit of the actual value.

III. RESULTS AND DISCUSSIONS

Since we are considering a GaAs/Al_{0.3}Ga_{0.7}As QW, the effective parameters used are : m_e=0.067m₀, m_{h_z}=0.377m₀, m_{h_{xy}}=0.112m₀, ε=13.2 for the well and barrier materials. The conduction band off-set is 0.6.

Our results show that, in the absence of magnetic fields, there is only one bound state, the singlet M=0. This is in agreement with previous calculations [10].

In Figure 1 we show the binding energy of the X⁻ singlet (M=0) state , E_b(X⁻), as a function of the QW width for different levels of approximation. In all of them only the fundamental QW states are taken into account. The most important contribution is given by the s-like relative particle state. We obtain an excellent convergence for 8 values of the λ parameter (between 50 and 800 Å) what means a basis set with 36 Slater determinants. The results show the expected behavior with larger binding energies for the narrowest QWs. The highest value is reached for L ~ 30 Å where the charge confinement is maximum. For comparison we also show the results obtained using just one λ value for each relative particle function in which case they are the variational parameters. Adding the higher relative particle angular momenta to the basis set, but keeping M=0, we observe a binding energy increase of the order of 50%.

Let us first analyze the cases in which the term $-(\hbar^2/m_{hxy})\vec{p}_1 \cdot \vec{p}_2$ is neglected (Eq. (9)). Notice that this term has no contribution when only s-states are considered. The most important contribution of the nonzero angular momentum wavefunctions is related to the repulsive Coulomb interaction. The s-states favor the electrons being closer to the hole while the other ones favor the electrons to be far from each other. Although these

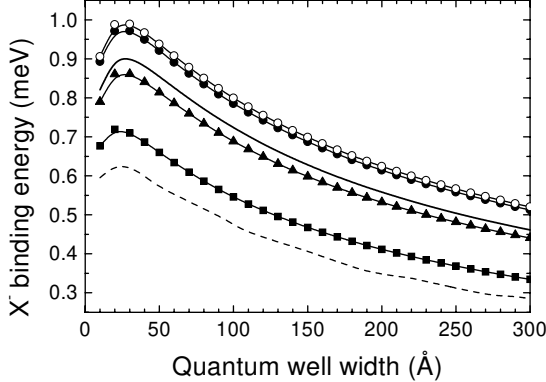


FIG. 1: X^- binding energy as a function of the QW width for different degrees of approximation: only s -states and one λ value for each relative particle function (dashed line), only s -states but with a set of 8 values of λ (squares), the same as before but including the p^\pm states contribution (triangles), full calculation including the d^\pm states contribution (full line). The two upper curves are equivalent to the last two, but neglecting the $-(\hbar^2/m_{hxy})\vec{p}_1 \cdot \vec{p}_2$ term (open circles include up to the d -states, while solid circles include only the s and p ones).

contributions are important, we obtain a good convergence adding only the p^\pm and d^\pm states to the basis set. Finally, when we add the repulsive $-(\hbar^2/m_{hxy})\vec{p}_1 \cdot \vec{p}_2$ term, a binding energy decrease of the order of 10% is observed. However, this does not change the fact that a basis with only p^\pm and d^\pm states is sufficient to obtain the convergence in the binding energy.

Figure 2a shows charged exciton binding energies obtained with different numbers of QW states in the basis set. In the case of X^- , what will be called full results takes into account two hole QW states and three electron ones which are enough to obtain a good convergence. The results with two electronic subbands present a discontinuity at 50 Å. At this width, the second QW solution for electrons becomes a QW bound state. As a result, there is an oscillator strength redistribution between the states inside and outside the QW. If an extra electron level is included in the basis this discontinuity is smoothed out. However, one can see that another discontinuity appears when the third

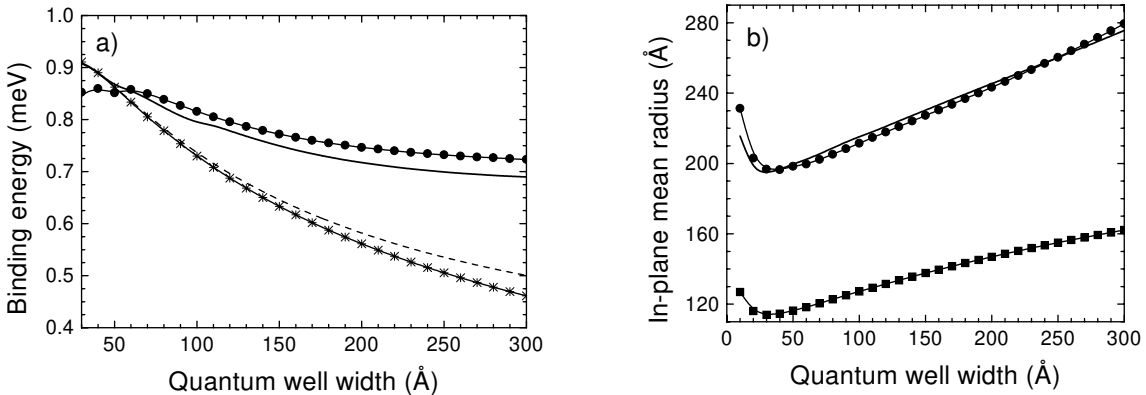


FIG. 2: (a) Charged exciton binding energy as a function of QW width. The X^- values were calculated using one electron and one hole subbands (stars), one electron and two hole subbands (dashed line), three electron and two hole subbands (full line). The X^+ results (circles) were obtained using three hole and two electron subbands. (b) Mean value of the in-plane relative particle radius for the exciton (squares), X^- (full line) and X^+ (circles) calculated with the complete basis.

QW solution for electrons becomes a bound state inside the well (100 Å). When a larger number of QW states is used, these discontinuities are completely smoothed out. This rises the numerical calculation efforts without a significant improvement of our results. The X^+ results are equivalent and only the full results are shown using two electron QW states and three hole ones (circles). As one can see in Fig. 2 the excited QW levels are important to describe the charged exciton fundamental state.

The main reasons for including more than one electron QW level in the charged exciton basis are the correlation and exchange effects. The QW hole subbands are energetically nearer than the electronic ones favoring their coupling mainly for wide QWs. This effect can be noticed in Fig. 2a. The inclusion of the second QW even solution for holes gives rise to a binding energy gain of the order of 9% for the largest quantum well. The electron contributions are more delicate : in the exciton case, the electron QW ground state already gives us the binding energy convergence. However,

this is not the case for the X^- . The particle interchange symmetry requires a flexible basis which can not be limited to the fundamental electron QW state. In the case of a 300 Å quantum well width, the full calculation increases the X^- binding energy by 40% comparing with the case where two hole and only one electron QW levels are taken into account. Nevertheless, there are two aspects that should be pointed out. One is that if more than one electron QW level is considered, the coupling between the even and odd QW solutions is allowed. The other is that the exciton binding energy is almost one order of magnitude larger than the charged exciton one.

One can see in Fig. 2a that as the QW is getting wider, the charged exciton becomes more weakly bound due to the effective one dimensional confinement decrease. The heavy hole is more localized by the quantum well potential than the electrons. Because of this, for QW widths less than 60 Å the strong overlap between the two holes of the X^+ enhances the Coulomb repulsion and the positively charged exciton is less bound than the negative one. For wider QWs, the less effective confinement and the hole subbands coupling lead the X^+ and X^- to present similar binding energies. This is in agreement with the experimental results of Glasberg *et al.* [6] and Finkelstein *et al.* [16].

Figure 2b shows the mean value of the in-plane relative particle radius for X^- and X^+ . As expected, the lower the binding energy of the complex, the larger its in-plane relative particle radius. These values should be compared to the exciton ones which is a much smaller complex. As a consequence, the charged exciton is more sensitive to interface defects than the neutral exciton. This result should be taken into account when considering the comparison with experimental results.

We compare our results with experimental ones in Fig. 3. Although the calculated binding energies are always lower than the experimental ones, it is important to realize that in the wide QW limit they are in good agreement. It is known that the sample structural defects increase the charged exciton binding energy and they are less important for wide QWs where the wavefunctions amplitudes are lower at the interfaces. Therefore, we attribute the results discrepancy to the effects of interface defects (Riva *et al.*[10]).

Most of the samples where the trions have been observed are one-side modulation

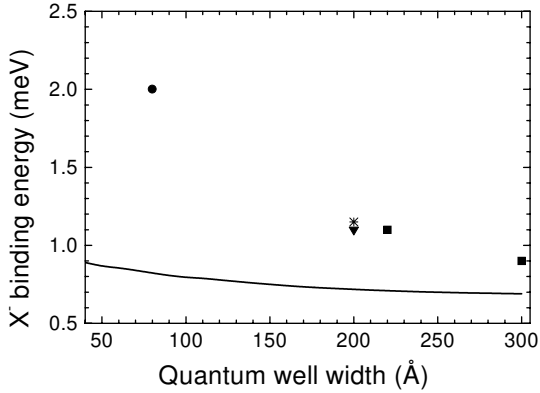


FIG. 3: X^- binding energy as a function of QW width. The solid line corresponds to our full calculation. The points are experimental data from: Glasberg et al.[6] (down triangle), Finkelstein et al. [16] (star), Yan et al.[17] (circle) and Shields et al.[18] (squares).

doped. This is made in order to improve the optical characteristics of the QW. As a consequence, they have an in-built electric field along the growth direction. To get a clearer idea about this effect on the trion binding energy, we considered the presence of an electric field applied along the z-direction. In Fig. 4, we show the X^- binding energy, (a), and the in-plane mean radius, (b), as a function of the longitudinal electric field. Three QW widths are considered: 100 Å (solid line), 200 Å (stars) and 300 Å (dashed line). The charge confinement is stronger for the narrowest well. In this case, the electric field effects are weaker. It is interesting to observe that the X^- binding energy increases slightly for fields up to 10 kV/cm. At higher values of electric field, the carriers wavefunctions begin to be localized at opposite QW interfaces. This phenomenon enhances the Coulomb repulsion at the same time that the attraction is weakened. For larger QWs, the electric field has a more important contribution and the X^- binding energy decreases quickly. In this situation, the confinement is less effective and the carriers are more easily localized at opposite QW interfaces. As a consequence, the initial X^- binding energy increase is observed at lower electric fields for 200 and 300 Å QW widths (see Fig. 5). For a 300 Å quantum well width the X^- becomes unbound for electric fields higher than 30

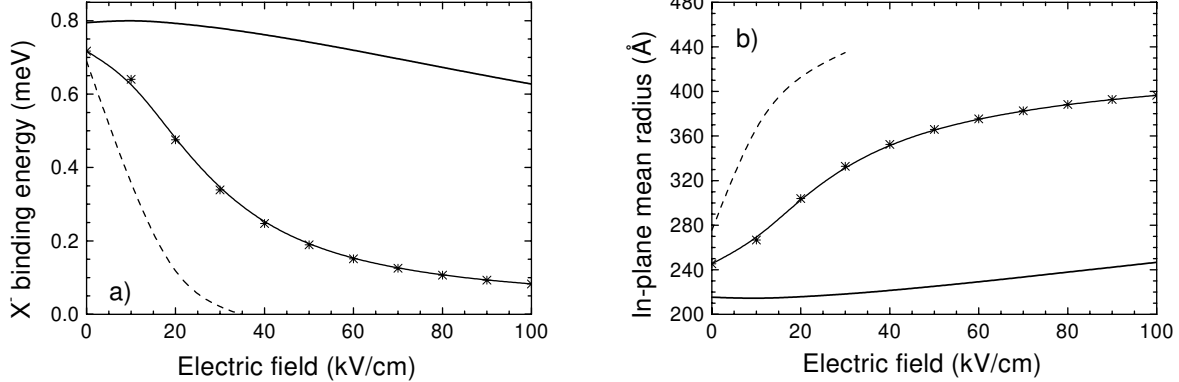


FIG. 4: (a) X^- binding energy as a function of longitudinal electric field for a 100 \AA QW width (solid line), 200 \AA QW width (stars) and 300 \AA QW width (dashed line) and (b) mean value of the in-plane relative particle radius.

kV/cm, a result not observed for excitons in similar conditions[19]. The X^+ has the same qualitative behaviors (not shown), but it becomes unbound only for electric fields higher than 40 kV/cm in the case of a 300 \AA QW width. It is important to remind that in all cases, the trion is an unbound state since, in the presence of longitudinal electric fields, the QW does not hold any carrier bound state in the strict sense. However, just as for the exciton case, the QWs present strong resonances with a long lifetime enabling its optical detection. As a general trend, the relative particle coordinates increase their average values for higher electric fields (Fig. 4b). It is also interesting to notice that the initial binding energy increase for the 100 \AA QW is accompanied by a slight relative particle radius reduction. In actual samples, the in-built electric field is rather small.

Figure 5 shows a comparison between our results and the experimental data from Shields *et al.*[20]. One can see that the agreement is better for higher electric field values when the positive and negative carriers are more spatially separated and the repulsion dominates over the attraction. It is known that the QW interfaces do not get the same quality during the growth process. The longitudinal electric field pushes the electrons, which are more sensitive to interface defects, toward the *good* interface.

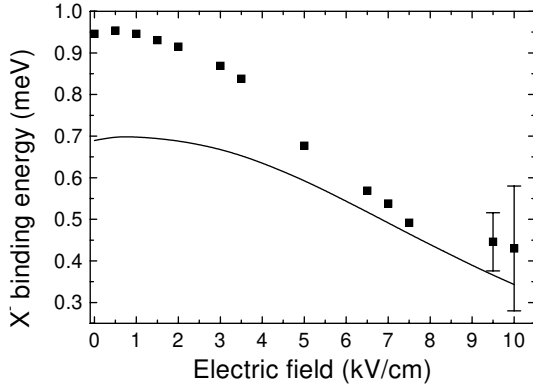


FIG. 5: X^- binding energy as a function of longitudinal electric field for a 300 Å quantum well width. The solid line corresponds to our full calculation. The squares are experimental data from Shields *et al.* [20]. The experimental error bars are shown for the two last points. At lower electric field values, the error bars are not significant.

Consequently, the good agreement at higher electric field values may indicate again that the main reason for the experimental and theoretical results discrepancy is the presence of structural imperfections. Another interesting point is the experimental observation of the slight X^- binding energy increase for low electric field values. This shows that our approximations retains the most important physical characteristics of the complex.

IV. CONCLUSION

In conclusion, we variationally calculated the trion binding energy in GaAs/Al_{0.3}Ga_{0.7}As semiconductor QWs. We showed that a flexible trial wavefunction, including the z-related degree of freedom, is required to obtain accurate results. In the presence of a longitudinal electric field, we observe the trion ionization for wide QWs. We believe that the interface defects have an important role in the trion dynamics, especially in the narrow QW and low field limits.

V. ACKNOWLEDGEMENTS

This work is supported by FAPESP (Brazil) and CNPq (Brazil).

REFERENCES

- [1] M. A. Lampert, Phys. Rev. Lett. **1**, 450 (1958).
- [2] G. Munsch and B. Stébé, Phys. Status Solidi (b) **64**, 213 (1974).
- [3] B. Stébé and A. Ainane, Superlattices Microstruct. **5**, 545 (1989).
- [4] K. Kheng, R. T. Cox, Y. Merle d'Aubigné, Franck Bassani, K. Saminadayar and S. Tatarenko, Phys. Rev. Lett. **71**, 1752 (1993).
- [5] G. Finkelstein, V. Umansky, I. Bar-Joseph, V. Ciulin, S. Haacke, J. -D. Ganiere and B. Deveaud, Phys. Rev. B **58**, 12637 (1998).
- [6] Shmuel Glasberg, Gleb Finkelstein, Hadas Shtrikman and Israel Bar-Joseph, Phys. Rev. B **59**, R10425 (1999).
- [7] A. B. Dzyubenko and A. Yu. Sivachenko, Phys. Rev. Lett. **84**, 4429 (2000).
- [8] C. Riva, F. M. Peeters and K. Varga, Phys. Rev. B **63**, 115302-1 (2001).
- [9] D. M. Whittaker and A. J. Shields, Phys. Rev. B **56**, 15185 (1997).
- [10] C. Riva, F. M. Peeters and K. Varga, Phys. Rev. B **61**, 13873 (2000).
- [11] R. McWeeny and B. T. Sutcliffe, *Methods of Molecular Quantum Mechanics* (Academic Press, London, 1969).
- [12] J. A. Brum, C. Priester, and G. Allan, Phys. Rev. B **32**, 2378 (1985).
- [13] C. Aldrich and R. L. Greene, Phys. Status Solidi (b) **93**, 343 (1979).
- [14] C. Prieter, G. Bastard, G. Allan and M. Lannoo, Phys. Rev. B **30**, 6029 (1984).
- [15] J. A. Brum and P. Hawrylak, Comments Cond. Mat. Phys. **18**, 135 (1997).
- [16] G. Finkelstein, H. Shtrikman, I. Bar-Joseph, Phys. Rev. B **53**, R1709 (1996)
- [17] Z. C. Yan, E. Goovaerts, C. Van Hoof, A. Bouwen, G. Borghs, Phys. Rev. B **52**, 5907 (1995)
- [18] A. J. Shields, M. Pepper, D. A. Ritchie, M. Simmons and G. A. C. Jones, Phys. Rev. B **51**, 18049 (1995)

- [19] J. A. Brum and G. Bastard, Phys. Rev. B **31**,3893 (1985).
- [20] A. J. Shields, F. M. Bolton, M. Y. Simmons, M. Pepper and D. A. Ritchie, Phys. Rev. B **55**, R1970 (1997)

Capítulo 3

Éxcitons carregados na presença de campos magnéticos longitudinais

1) INTRODUÇÃO

Este capítulo tem por objetivo apresentar o tratamento teórico que nós utilizamos para representar a dinâmica do X^- no limite de fracos campos magnéticos longitudinais (entre 0 e 6 T). Isto significa campos magnéticos geradores de uma energia ciclotrônica menor ou comparável à interação coulombiana entre as cargas.

A exemplo do trabalho realizado no caso da ausência de campos magnéticos, nós utilizamos o método variacional para cálculo da energia de ligação do X^- . Novamente empregamos uma base não ortogonal de determinantes de Slater com funções gaussianas para os orbitais de partícula relativa no plano xy.

De forma geral, foram preservados os mesmos parâmetros, a mesma nomenclatura e o mesmo sistema de coordenadas do caso de campo magnético nulo. A diferença essencial está na descrição do centro de massa do X^- através de níveis de Landau. Sendo este uma partícula carregada, sofre a ação do campo magnético longitudinal não podendo ser descrito como uma partícula livre. Este “grau de liberdade adicional” é responsável por uma série de efeitos interessantes, em especial, a existência de um estado tripleno ligado.

2) ÉXCITON COM CAMPO MAGNÉTICO

O Hamiltoniano do exciton em coordenadas absolutas e na presença de um campo magnético é escrito como :

$$H = \frac{1}{2m_e} \left(\vec{p}_e + \frac{e}{c} \vec{A}_e \right)^2 + \frac{1}{2m_h} \left(\vec{p}_h - \frac{e}{c} \vec{A}_h \right)^2 + V_e(z_e) + V_h(z_h) - \frac{e^2}{\epsilon |\vec{r}_e - \vec{r}_h|} \quad (1)$$

onde : * \vec{A}_e (\vec{A}_h) é o potencial vetor para o elétron (buraco)

* V_e (V_h) é o potencial do poço quântico para elétrons (buracos)

* a carga (e) é tomada positiva

Consideraremos o campo magnético paralelo à direção z (longitudinal) e usaremos o calibre de Coulomb, onde :

$$\vec{A} = \frac{1}{2} \vec{B} \times \vec{r} = \frac{1}{2} B(-y, x, 0) \quad (2)$$

e

$$\left[\vec{p}, \vec{A} \right] = 0 \quad (3)$$

Como os potenciais vetores para elétron e buraco não possuem componentes na direção z, podemos separar o Hamiltoniano em termos referentes à direção z e ao plano xy (a menos da interação coulombiana).

$$H = \frac{1}{2m_e} \left(\vec{p}_{exy} + \frac{e}{c} \vec{A}_e \right)^2 + \frac{1}{2m_{hxy}} \left(\vec{p}_{hxy} - \frac{e}{c} \vec{A}_h \right)^2 + \frac{1}{2m_e} p_{ez}^2 + V_e(z_e) + \frac{1}{2m_{hz}} p_{hz}^2 + V_h(z_h) - \frac{e^2}{\epsilon |\vec{r}_e - \vec{r}_h|} \quad (4)$$

Usando a transformação de centro de massa e partícula relativa usuais no plano xy (coordenadas polares):

$$\begin{aligned} \vec{R} &= \frac{\vec{m}_e \vec{\rho}_e + m_{hxy} \vec{\rho}_h}{m_e + m_{hxy}} \\ \vec{\rho} &= \vec{\rho}_e - \vec{\rho}_h \end{aligned} \quad (5)$$

chegamos a :

$$\begin{aligned}
H = & \left(\frac{1}{2m_e} p_{ez}^2 + V_e(z_e) \right) + \left(\frac{1}{2m_{hz}} p_{hz}^2 + V_h(z_h) \right) + \\
& \frac{\vec{P}}{2M} + \frac{\vec{p}}{2\mu} + \frac{e}{c} \left\{ \frac{\vec{A}_\rho \bullet \vec{P}}{M} + \frac{\vec{A}_R \bullet \vec{p}}{\mu} + \left(\frac{1}{m_e} - \frac{1}{m_{hxy}} \right) \vec{A}_\rho \bullet \vec{p} \right\} + \\
& \frac{e^2}{2c^2} \left\{ \frac{\vec{A}_R}{\mu} + 2 \left(\frac{1}{m_e} - \frac{1}{m_{hxy}} \right) \vec{A}_R \bullet \vec{A}_\rho + \frac{1}{M^2} \left(\frac{m_e^2}{m_{hxy}} + \frac{m_{hxy}^2}{m_e} \right) \vec{A}_\rho^2 \right\} \\
& - \frac{e^2}{\epsilon \sqrt{\rho^2 + (z_e - z_h)^2}}
\end{aligned} \tag{6}$$

onde : * $M = m_e + m_{hxy}$ é a massa do centro de massa e \vec{P} é seu momento linear

* $\mu = m_e \cdot m_{hxy}/M$ é a massa reduzida e \vec{p} é o momento linear da partícula relativa

* $\vec{A}_\rho = \frac{1}{2} \vec{B} \times \vec{\rho}$ é o potencial vetor da partícula relativa

* $\vec{A}_R = \frac{1}{2} \vec{B} \times \vec{R}$ é o potencial vetor do centro de massa

O centro de massa do exciton é neutro, logo não sofre a ação do campo magnético e uma transformação unitária elimina de (6) os termos proporcionais a \vec{A}_R . Esta transformação é [1] :

$$F = \exp \left(\frac{ie}{\hbar c} \vec{A}_\rho \bullet \vec{R} \right) \tag{7}$$

Aplicando a transformação unitária (7) sobre o Hamiltoniano (6) obtemos :

$$\begin{aligned}
H' = & \left(\frac{1}{2m_e} p_{ez}^2 + V_e(z_e) \right) + \left(\frac{1}{2m_{hz}} p_{hz}^2 + V_h(z_h) \right) + \\
& \frac{\vec{P}}{2M} + \frac{2e}{Mc} \vec{A}_\rho \bullet \vec{P} + \frac{e^2}{2\mu c^2} \vec{A}_\rho^2 + \frac{e}{c} \left(\frac{1}{m_e} - \frac{1}{m_{hxy}} \right) \vec{A}_\rho \bullet \vec{p} + \frac{\vec{p}}{2\mu} + \\
& - \frac{e^2}{\epsilon \sqrt{\rho^2 + (z_e - z_h)^2}}
\end{aligned} \tag{8}$$

O centro de massa é uma partícula livre pois o campo magnético não atua sobre ele, sendo então descrito por uma onda plana com vetor de onda \vec{K}_R . Consequentemente, as duas primeiras parcelas da segunda linha de (8) não contribuem para o estado fundamental do sistema ($\vec{K}_R = 0$).

É importante ressaltar que como estamos calculando a energia de ionização do exciton, a energia do par elétron-buraco não interagente ($E = \frac{\hbar e B}{2\mu c}$) deve ser tomada como o zero da energia de ligação.

3) X⁻ COM CAMPO MAGNÉTICO

Nos cálculos para o X⁻ também utilizamos o calibre de Coulomb (2,3), mas a transformação de coordenadas no plano xy deve levar em consideração a presença de mais um elétron :

$$\vec{R} = \frac{m_e (\vec{\rho}_{e1} + \vec{\rho}_{e2}) + m_{hxy} \vec{\rho}_h}{2m_e + m_{hxy}} \quad (9)$$

$$\vec{\rho}_i = \vec{\rho}_{ei} - \vec{\rho}_h \quad i=1,2$$

Analogamente definimos os potenciais vetores :

$$\vec{A}_R = \frac{1}{2} \vec{B} \times \vec{R} \quad \text{e} \quad \vec{A}_{\rho_i} = \frac{1}{2} \vec{B} \times \vec{\rho}_i \quad \text{onde } i=1,2 \quad (10)$$

A obtenção do equivalente ao Hamiltoniano (4) para o X⁻ é feita pela simples adição de mais um elétron à expressão, gerando mais um termo de atração coulombiana e um novo de repulsão. O Hamiltoniano em termos das coordenadas de centro de massa e partículas relativas é obtido de forma completamente análoga ao caso do exciton.

O nosso sistema apresenta conservação do momento linear conjugado generalizado [2,3] no plano xy, ou seja, o operador

$$\vec{\Pi} = \vec{P} - \frac{e}{c} \left\{ \vec{A}_R + \left(1 - \frac{m_e}{M} \right) \left(\vec{A}_{\rho 1} + \vec{A}_{\rho 2} \right) \right\} \quad (11)$$

comuta com o Hamiltoniano (note que agora M é a massa do centro de massa do X'). Este momento desempenha o mesmo papel que o momento total no caso do exciton e raramente é possível eliminar um grau de liberdade do problema através de uma transformação unitária. Neste caso, no entanto, as componentes x e y de (11) não comutam entre si. Escolheremos uma delas (x) como bom número quântico.

A autofunção de Π_x é dada por :

$$f = \exp \left\{ \frac{i}{\hbar} \left[\vec{q} + \frac{e}{c} \left(1 - \frac{m_e}{M} \right) \left(\vec{A}_{\rho 1} + \vec{A}_{\rho 2} \right) \right] \bullet \vec{R} - \frac{ie}{2\hbar c} B Y_{CM} . X_{CM} \right\} \quad (12)$$

onde $\vec{q} = (q_x, 0, 0)$ para q_x sendo o autovalor de Π_x .

As autofunções do Hamiltoniano são também de Π_x e como Π_x tem um operador de derivação sobre a coordenada de centro de massa X_{CM} , podemos escrever as autofunções do Hamiltoniano que descrevem a dinâmica no plano xy na forma :

$$\Psi(X_{CM}, Y_{CM}, x_1, x_2, y_1, y_2) = f . \Phi(Y_{CM}, x_1, x_2, y_1, y_2) \quad (13)$$

Temos então que (12) é a transformação unitária que aplicada sobre o Hamiltoniano resolve a coordenada X_{CM} retirando das funções a dependência desta.

O Hamiltoniano transformado do X' é dado por :

$$\begin{aligned} H' = & H(z) + V_C + \frac{1}{2M} \left[\vec{P} + \frac{e}{c} \left(\vec{A}_R - \vec{C} \right) \right]^2 + \frac{2e^2}{c^2 M} \left(1 - \frac{m_e}{M} \right) \left(\vec{A}_R - \vec{C} \right) \bullet \left(\vec{A}_{\rho 1} + \vec{A}_{\rho 2} \right) + \\ & \frac{2e}{cM} \left(1 - \frac{m_e}{M} \right) \left(\vec{A}_{\rho 1} + \vec{A}_{\rho 2} \right) \bullet \vec{P} + \frac{1}{2\mu} \left(\vec{p}_1^2 + \vec{p}_2^2 \right) + \frac{e}{c} \left(\frac{1}{m_e} - \frac{m_e}{M\mu} \right) \left(\vec{A}_{\rho 1} \bullet \vec{p}_1 + \vec{A}_{\rho 2} \bullet \vec{p}_2 \right) + \\ & - \frac{e.m_e}{cM\mu} \left(\vec{A}_{\rho 1} \bullet \vec{p}_2 + \vec{A}_{\rho 2} \bullet \vec{p}_1 \right) + \frac{e^2}{2c^2 M^2} \left(\frac{m_e^2}{m_{hxy}} + \frac{m_{hxy}^2}{m_e} + 2m_e + 2m_{hxy} \right) \left(\vec{A}_{\rho 1}^2 + \vec{A}_{\rho 2}^2 \right) + \\ & \frac{e^2}{c^2 M^2} \left(\frac{m_e^2}{m_{hxy}} - 2m_e - 2m_{hxy} \right) \left(\vec{A}_{\rho 1} \bullet \vec{A}_{\rho 2} \right) + \frac{3e^2}{2c^2 M} \left(1 - \frac{m_e}{M} \right)^2 \left(\vec{A}_{\rho 1} + \vec{A}_{\rho 2} \right)^2 + \frac{1}{m_{hxy}} \vec{p}_1 \bullet \vec{p}_2 \end{aligned} \quad (14)$$

onde $\vec{C} = \frac{B}{2}(Y_{CM}, X_{CM}, 0)$, $H(z)$ é o Hamiltoniano do poço quântico, V_C são os termos de

interação coulombiana e os termos proporcionais ao vetor \vec{q} foram considerados nulos pois buscamos o estado fundamental do sistema onde $q_x=0$.

Note que a terceira parcela de (14) é um oscilador harmônico para o centro de massa (níveis de Landau) pois como a função Φ (13) não depende de X_{CM} temos que o operador

$$\frac{e}{cM} \left(\vec{A}_R - \vec{C} \right) \bullet \vec{P} \text{ é nulo.}$$

As duas parcelas seguintes são os termos de acoplamento entre o movimento do centro de massa e o movimento das partículas relativas. Seus elementos de matriz só serão não nulos quando calculados entre níveis de Landau com paridades distintas, ou seja, considerando um único nível de Landau, os movimentos do centro de massa e das partículas relativas são desacoplados. Isto sugere escrever a função de onda como :

$$\Phi(Y_{CM}, x_1, x_2, y_1, y_2) = \varphi(x_1, x_2, y_1, y_2) \cdot \sum_n \Lambda_n(Y_{CM}) \quad (15)$$

onde $\Lambda_n(Y_{CM})$ é a autofunção do n -ésimo nível de Landau de uma partícula carregada.

Vale ressaltar que o acoplamento entre níveis de Landau do centro de massa ocorre quando simultaneamente :

- a) os níveis de Landau têm paridades distintas
- b) o momento angular total das partículas relativas difere por ± 1 entre os níveis de Landau que se acoplam

Este resultado mostra que a aproximação de um único nível de Landau, freqüentemente utilizada em outros trabalhos [2], despreza termos que podem desempenhar um papel significativo.

4) RESULTADOS E DISCUSSÕES

A figura 1 mostra a energia de ligação dos estados tipo singuleto ($M=0$) e triploto ($M=-1$) do X^- em função do campo magnético longitudinal para um poço quântico de 200 Å. Fica clara a importância do segundo nível de Landau do centro de massa na dinâmica do

X^- . Em especial, o triplete ($M=-1$) só é um estado ligado quando o campo magnético é não nulo e o segundo nível de Landau é levado em conta. Devemos ressaltar que os únicos estados ligados na presença de um campo magnético longitudinal (até 10 T) são o singuleto com a componente z do momento angular total de partícula relativa nula ($M=0$) e o triplete com $M=-1$. A convergência dos valores calculados é alcançada já com o segundo nível de Landau do centro de massa.

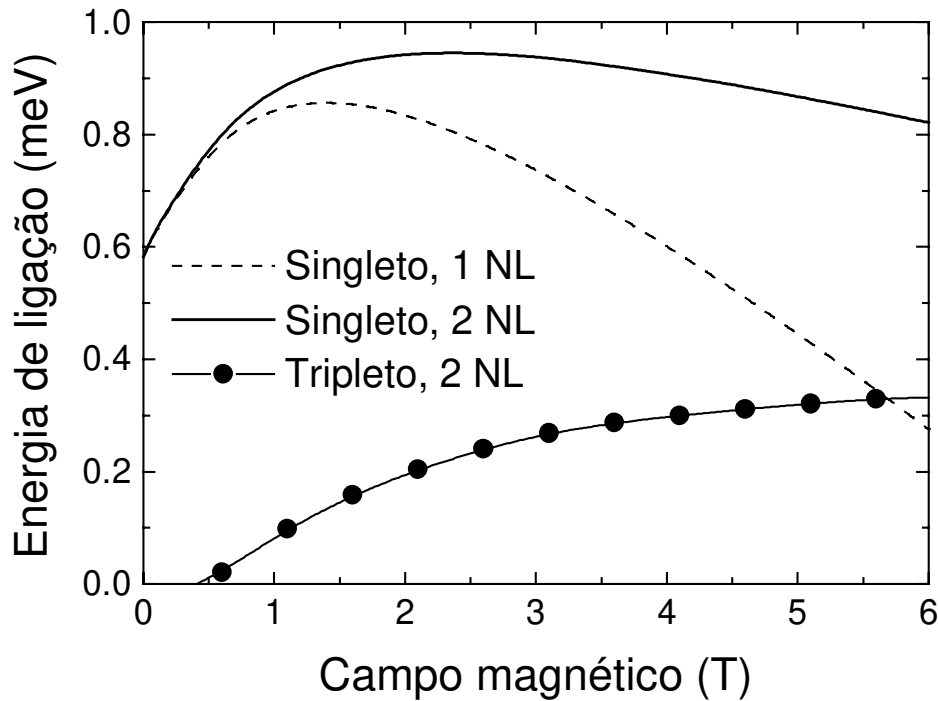


Figura 1 – Energia de ligação do X^- singuleto ($M=0$) e triplete ($M=-1$) em função do campo magnético para os estados ligados com 1 ou 2 níveis de Landau do centro de massa (NL). $L = 200 \text{ \AA}$ e 2 níveis de poço de buraco pesado foram considerados.

O efeito principal do aumento do campo magnético é a diminuição das órbitas das cargas e consequente encurtamento dos orbitais de partícula relativa. Esta aproximação entre as cargas favorece tanto a atração quanto a repulsão coulombianas. Inicialmente a atração é a interação mais favorecida aumentando a energia de ligação do X^- , mas a partir de 1.5 T (um nível de Landau) ou 2.5 T (dois níveis de Landau) o fortalecimento da repulsão

coulombiana gera uma diminuição da energia de ligação do singuleto. No caso do triplete, este efeito se manifesta através da estabilização da energia de ligação.

A figura 2 mostra a energia de ligação do singuleto ($M=0$) e do triplete ($M=-1$) do X^- em função da largura do poço na presença de um campo magnético de 5 T. Percebemos que o singuleto e o triplete do X^- têm energias de ligação que evoluem de forma diferente em função da largura do poço para um certo valor de campo magnético.

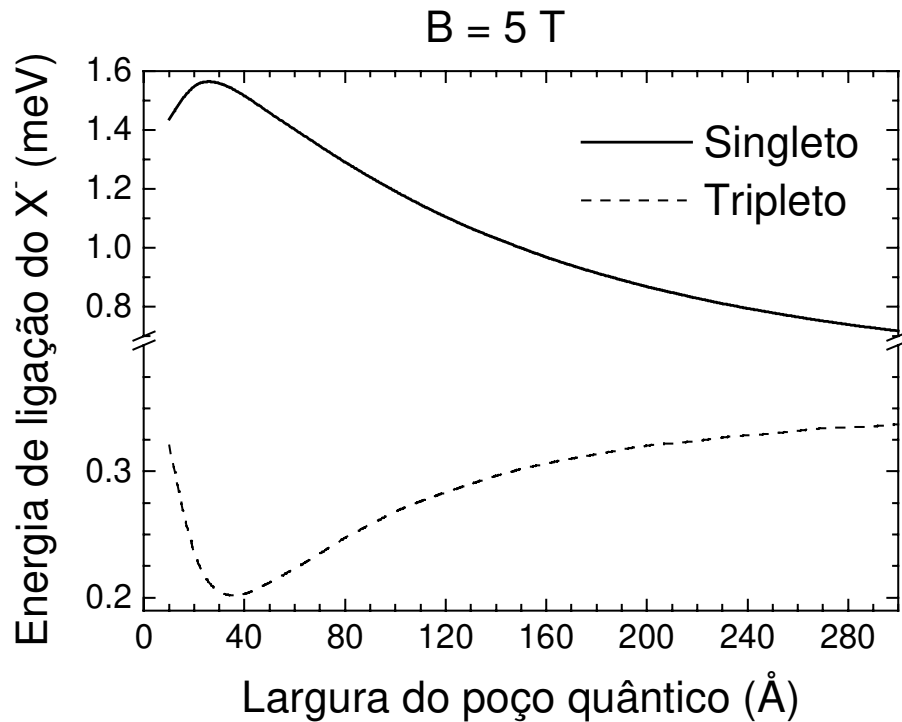


Figura 2 – Energia de ligação do X^- singuleto ($M=0$) e triplete ($M=-1$) em função da largura do poço quântico para um campo magnético de 5 T. Foram considerados 2 níveis de Landau e dois de buraco pesado.

No limite de poços bem estreitos o X^- tende a se comportar como no “bulk” do material da barreira e no limite de poços largos ele tende ao comportamento no “bulk” do material do poço. Há uma região intermediária onde o confinamento das cargas é muito importante. Nesta região, o comportamento do singuleto e do triplete do X^- , em função da largura do poço, são bem distintos. Isto se deve ao fato de que a simetria espacial do triplete anula a função de onda caso as coordenadas de partículas relativas tendam a ser as mesmas.

Podemos então falar de uma “repulsão intrínseca” entre as partículas relativas no caso do triplete. Esta é a razão pela qual a energia de ligação do triplete aumenta para poços mais largos. No caso do singuleto não existe esta “repulsão intrínseca” e o comportamento oposto é verificado.

Outro reflexo da simetria espacial dos estados tipo triplete pode ser visto na figura 3 onde apresentamos a energia de ligação do triplete ($M=-1$) do X^- em função do campo elétrico longitudinal para $L=100 \text{ \AA}$, $L=200 \text{ \AA}$, $L=300 \text{ \AA}$ e um campo magnético de 1 T. A separação das cargas devido ao campo elétrico provoca um aumento da energia de ligação do triplete no caso de $L=100 \text{ \AA}$. Para o poço mais largo, o enfraquecimento da atração coulombiana e simultâneo aumento da repulsão induzidos pelo campo elétrico provoca diminuição da energia de ligação mesmo para o estado triplete. O caso $L=200 \text{ \AA}$ aparece como uma situação intermediária. No caso do estado singuleto ($M=0$), a presença de um campo elétrico longitudinal diminui a energia de ligação do X^- para todas as larguras de poço anteriormente consideradas para o caso do estado triplete ($M=-1$). Estes resultados podem ser vistos na figura 4 onde consideramos as mesmas condições da figura 3 só que para o estado singuleto ($M=0$).

A figura 5 mostra a energia de ligação do X^- em função do campo magnético considerando a ausência de campo elétrico e a presença de um no valor de 10 kV/cm. O estado triplete apresenta uma fraca dependência com o campo elétrico quando comparado ao estado singuleto. Os efeitos são mais significativos para campos mais altos quando a repulsão coulombiana é reforçada.

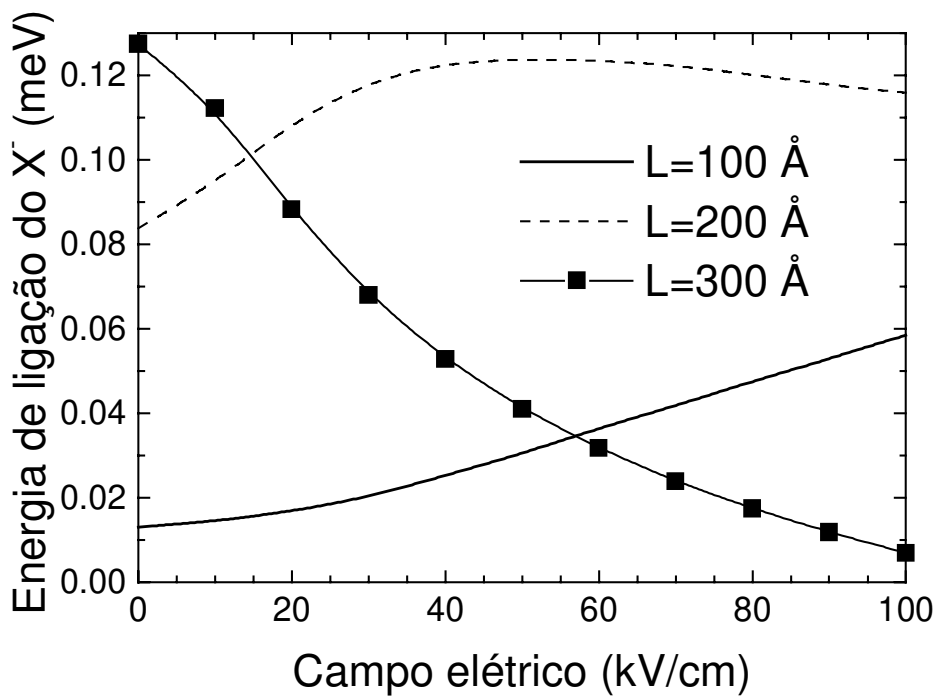


Figura 3 – Energia de ligação do X^- triplo ($M=-1$) em função do campo elétrico longitudinal para $L=100 \text{ \AA}$, $L=200 \text{ \AA}$ e $L=300 \text{ \AA}$ e um campo magnético de 1 T. Foram considerados 2 níveis de Landau e dois de buraco pesado.

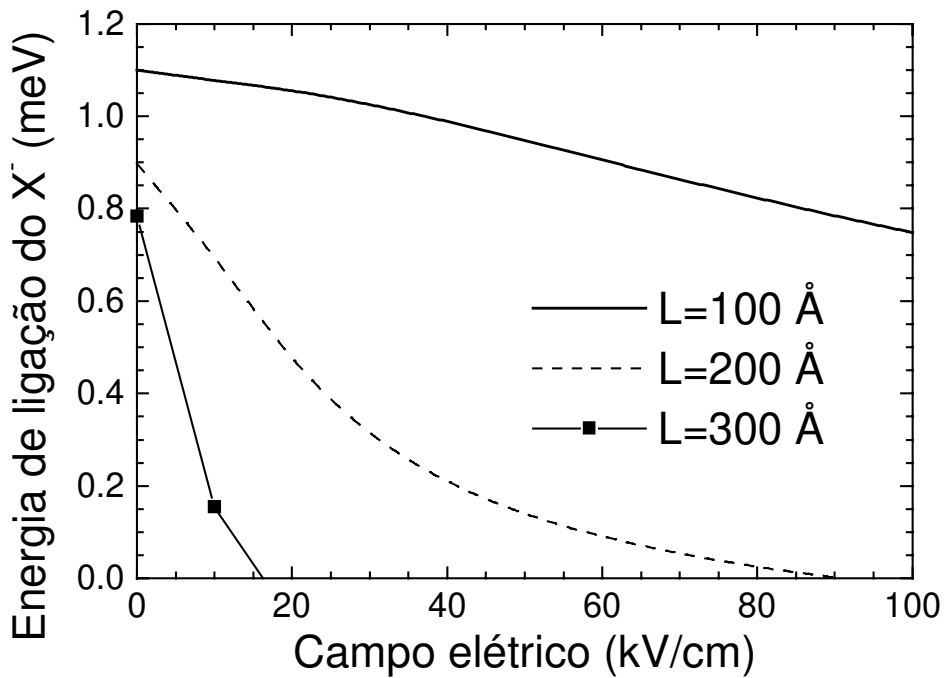


Figura 4 – Mesmo da figura 3, mas para os estados singlete ($M=0$).

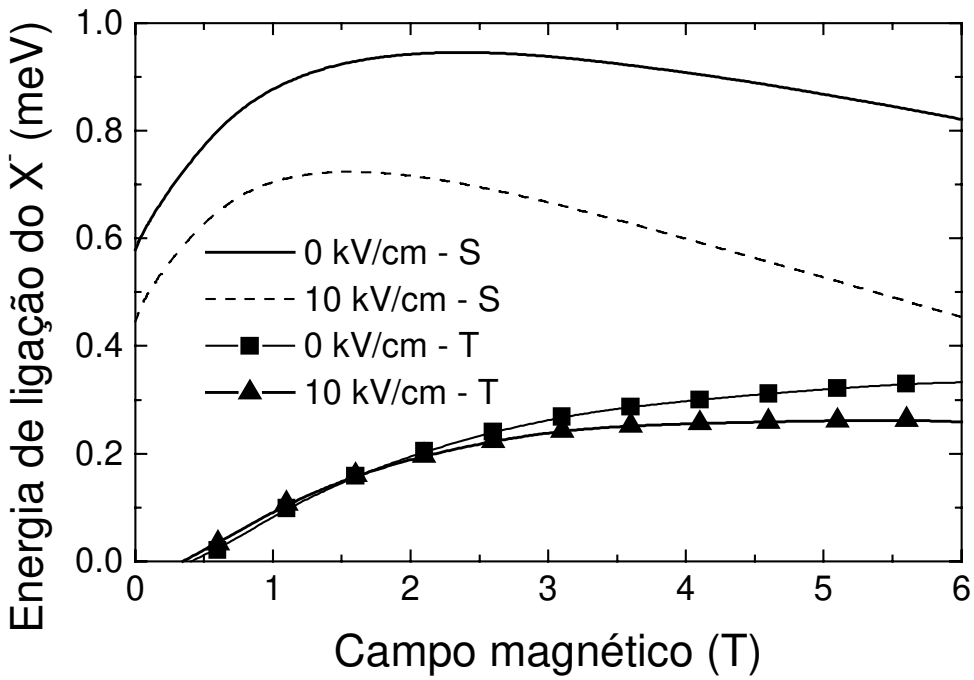


Figura 5 – Energia de ligação do X^- em função do campo magnético longitudinal para $F=0$ kV/cm e 10 kV/cm. “S” indica estado singuleto ($M=0$) e “T” indica estado tripleto ($M=-1$). Foram considerados 2 níveis de Landau e dois de buraco pesado.

A figura 6 mostra a comparação de nossos resultados com os obtidos experimentalmente [4]. Podemos perceber que os valores teóricos obtidos são sempre inferiores aos experimentais. O que mais chama a atenção, no entanto, é a discordância qualitativa entre os resultados. Os valores experimentais para o singuleto não apresentam nenhum sinal de diminuição da energia de ligação com o campo magnético, o que se verifica para valores de campo maiores que 2 T no caso dos resultados teóricos. Esta discordância é ainda maior no caso do estado tripleto.

Os resultados apresentados aqui foram obtidos com uma base que considera apenas o estado fundamental do poço de potencial para elétrons. A importância dos níveis eletrônicos excitados para a descrição da dinâmica do X^- na presença de campos magnéticos já é conhecida [5] e a inclusão destes na base é obviamente o passo seguinte na tentativa de obter uma melhor concordância entre teoria e experimento.

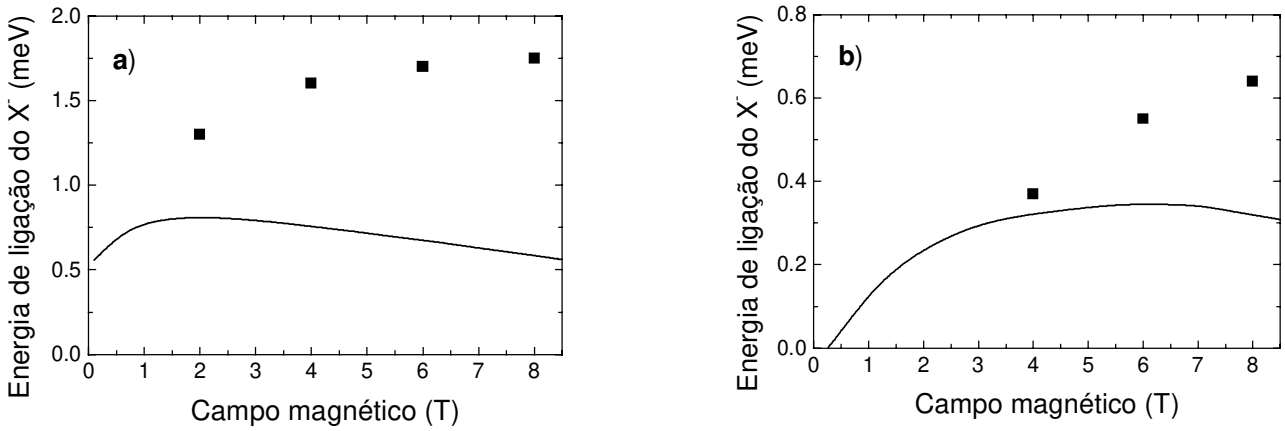


Figura 6 – Energia de ligação do X^- em função do campo magnético para o estado singuleto com $M=0$ (a) e tripleno com $M=-1$ (b) em um poço quântico com $L=300\text{ \AA}$. Os quadrados correspondem a dados experimentais [4].

Esta ampliação da base é um processo extremamente delicado devido à indistingibilidade dos elétrons, mas foi realizado com sucesso para o caso da ausência de campos magnéticos. Quando estes campos são considerados, a parte da função variacional referente ao centro de massa passa a ser descrita por níveis de Landau com intrincadas regras de acoplamento. Isto aumenta enormemente o tamanho da matriz a ser diagonalizada em comparação com o caso de campo magnético nulo, trazendo dificuldades adicionais, principalmente relacionadas à inversão numérica da matriz de superposição durante o processo de diagonalização do Hamiltoniano. Apesar de nossos esforços, não conseguimos contornar os problemas numéricos que surgiram quando a base usada considerava mais que o estado fundamental do poço de elétrons. Este cálculo permanece em aberto.

Os resultados teóricos obtidos por Riva *et al.* [6] apresentam uma excelente concordância com os valores experimentais. Eles utilizam o *método variacional estocástico* com uma base de *funções gaussianas deformadas* tridimensionais onde a presença do potencial do poço quântico é considerada através de uma largura diferente para a direção z destas gaussianas. Apesar de obter melhores resultados, a base empregada é menos flexível que a nossa e bastante carente no que se refere a significado físico.

5) CONCLUSÕES

Mesmo não obtendo a concordância desejada com os resultados experimentais, alguns aspectos merecem ser ressaltados. Em primeiro lugar, nossos cálculos mostram que na presença de campos magnéticos longitudinais apenas os estados singlet com $M=0$ e tripleto com $M=-1$ são ligados, concordando com a experiência. Em segundo lugar, mostramos a importância do acoplamento entre a dinâmica do centro de massa e das partículas relativas através do efeito da inclusão do segundo nível de Landau do centro de massa na base.

A existência de estados tripleto ($M=-1$) opticamente ativos mostra que as interfaces dos poços não são simétricas [7]. Outro resultado importante é a saturação da energia de ligação do X^- com o aumento do campo magnético [8]. Este é um resultado de difícil compreensão se considerarmos o X^- formado por cargas livres. Tudo isto nos leva a ressaltar a importância dos defeitos de interface na completa descrição da dinâmica do X^- .

6) BIBLIOGRAFIA

- [1] R. Knox; *Theory of Excitons*, New York : Academic Press, 1963
- [2] B. Stébé, E. Feddi and G. Munsch, Phys. Rev. B **35**, 4331 (1987)
- [3] V. Édel'shtein, Sov. Phys. JETP **50**, 384 (1979)
- [4] A. J. Shields, M. Pepper, D. A. Ritchie, M. Simmons and G. A. C. Jones, Phys. Rev. B **51**, 18049 (1995)
- [5] D. M. Whittaker and A. J. Shields, Phys. Rev. B **56**, 15185 (1997).
- [6] C. Riva, F. M. Peeters and K. Varga, Phys. Rev. B **63**, 115302-1 (2001).
- [7] A. B. Dzyubenko and A. Yu. Sivachenko, Phys. Rev. Lett. **84**, 4429 (2000).
- [8] S. Glasberg, G. Finkelstein, H. Shtrikman and Israel Bar-Joseph, Phys. Rev. B **59**, R10425 (1999).

Capítulo 4

The interface defect influence on the ionization energy of charged excitons in semiconductor quantum wells

Luis C. O. Dacal^{1,2}, R. Ferreira¹, G. Bastard¹ and José A. Brum^{2,3}

(1) *Laboratoire de Physique de la Matière Condensée ENS ,*

24, rue Lhomond, 75005 -Paris, France,

(2) *IFGW-DFMC, Universidade Estadual de Campinas,*

C.P. 6165, 13083-970, Campinas-SP, Brazil, and

(3) *Laboratório Nacional de Luz Síncrotron - ABTLuS,*

C. P. 6192, 13084-971, Campinas-SP, Brazil

Abstract

We present a model to take into account the interface defects contribution to the ionization energy of charged excitons (trions). We use gaussian defect potentials and one particle gaussian basis set. All the Hamiltonian defect terms are analytically calculated for the s-like trial wavefunctions. The dependence of the ionization energy and of the trion size on the quantum well width and on the defect size are investigated using a variational method for GaAs/Al_{0.3}Ga_{0.7}As quantum wells. We show that even in the case of strictly structural defects the trion is more strongly affected than the exciton.

I. INTRODUCTION

The stability of charged excitons (trions) was firstly proposed by Lampert[1]. A charged exciton is a complex formed when there is an excess of charge in a semiconductor and an extra electron or hole is bound by the electrical dipole of a neutral exciton. In the first case we have a negative complex (X^-) and in the second case we have a positive one (X^+). These complexes are analogous to the ions H^- and H_2^+ in atomic physics. The advantage of working with semiconductor materials is that the screening of electrical interactions gives rise to the possibility of obtaining, with magnetic fields accessible in laboratories, cyclotron energies of the same order of the Coulomb ones while, in the H^- and H_2^+ cases, this is only possible in astrophysical systems. The first trion binding energy calculation[2] showed that its value is not large enough to be experimentally detected in semiconductor bulk materials. However, this value is one order of magnitude larger in semiconductor quantum wells[3]. This is a consequence of the carriers confinement inside the quantum well (QW) due to the energy gap difference between the barrier and well materials. The first experimental observation of a trion spectrum was made by Kheng *et al.*[4] in a II-VI type QW. In this case the trion binding energy is more than twice the value for III-V systems[5].

There has been an intense discussion in the literature about the influence of charge localization potentials on the trion experimental observations. Most of the theoretical results[6–8] shows weaker binding energies than that experimentally observed[9–12]. This suggests that the trion may be trapped by some kind of QW interface defect. Eytan *et al.*[13] presented experimental evidences of X^- localization due to electrostatic potential fluctuations generated by the ionized donors at the barrier material. Dzyubenko and Sivachenko[14] showed that the optical activity of the X^- triplet state can only be possible due to a QW symmetry break. On the other hand, results from time resolved photoluminescence indicate that the trion optical emission is dominated by free charged excitons[15].

To shed some light to this problem, we present a simple model to include the interface

defects contribution in the trion Hamiltonian. This kind of defect is always present at the QW interface due to the mixture of well and barrier materials during the QW growth process. The protrusion of a material with lower gap in the region with a greater one gives rise to structural defects that are attractive for both electrons and holes in type I QWs. The average in-plane (xy) trion radius is of the order of hundreds of angstroms meaning that it is strongly sensitive to this kind of defect.

II. MODEL

We consider a semiconductor QW, more exactly a GaAs layer grown between two Al_{0.3}Ga_{0.7}As layers. The carriers are confined in the GaAs layer. The effective mass and envelope function frameworks are used to describe the semiconductor materials and the QW respectively. We neglect the band bending and the effect of the excess of carriers due to the doping. The QW width is in the z-direction (growth direction). The valence and conduction subbands are approximated by parabolic dispersions what is less accurate for holes. Therefore, this approximation is more severe in the case of X⁺.

We start with the assumption that the QW confinement is strong enough to make a z and (x,y) separable wavefunction in the basis set reasonable. We use the noninteracting electron and hole solutions for ideal QWs as the z-part of the one particle trial wavefunctions. The continuum of states is emulated by a finite set of discrete states generated by a wider QW (1000 Å) with infinite barriers embedding the structure we are interested in.

The axial symmetry will be preserved by the defect potential. This leads us to use polar coordinates to describe the X⁻ in-plane motion in terms of center of mass (CM) and relative coordinates considering a physical picture : the X⁻ is composed by an exciton and a distant electron bound to its electrical dipole[8].

$$\vec{R} = \frac{m_e(\vec{\rho}_{e1} + \vec{\rho}_{e2}) + m_{hxy}\vec{\rho}_h}{M}$$

$$\vec{\rho}_1 = \vec{\rho}_{e1} - \vec{\rho}_h \quad (1)$$

$$\vec{\rho}_2 = \vec{\rho}_{e2} - \frac{m_e \vec{\rho}_{e1} + m_{hxy} \vec{\rho}_h}{m}$$

Here the electron mass is isotropic. On the other hand, the hole dispersion is strongly non-parabolic in QWs, but, as a first approximation, the off-diagonal terms of the Luttinger Hamiltonian can be neglected. In this case, the hole mass is anisotropic and shows a lighter in-plane value. Using this approximation, the X⁺ in-plane coordinates are easily obtained from the previous ones through the electron and hole labels interchange. The CM mass is given by $m_{hxy}+2m_e$. We use the same mass values for the well and the barrier materials.

Due to the presence of the defect, the CM is not a free particle. We label the trion state through the following good quantum numbers : the total angular momentum in the z direction (including the CM contribution), M , and the total relative coordinates spin, S ($S=S_1+S_2$), which allows us to separate the solutions in singlet and triplet states.

The two electrons (holes in the case of X⁺) indistinguishability leads us to use a Slater determinant basis. We assume that the internal degrees of freedom are not strongly affected by the defect potential[16, 17]. Consequently, the main effect of the interface roughness is the localization of the CM which is weakly coupled to the relative coordinates giving rise to a low increase in the ionization energy. In the absence of structural defects and external fields, only the singlet trion state ($M=0$) is a bound state. Therefore, we consider only this configuration and the orbital part of the charged exciton trial wavefunction is written as :

$$\Psi_0 = N_{i,j,m} \cdot \chi_0(z_h) \cdot \chi_0(z_{e1}) \cdot \chi_0(z_{e2}) \cdot \phi_m^0(\vec{R}) \times [\phi_i^0(\vec{\rho}_1)\phi_j^0(\vec{\rho}_2) + \phi_i^0(\vec{\rho}_3)\phi_j^0(\vec{\rho}_4)], \quad (2)$$

where $N_{i,j,m}$ is the determinant normalization, $\chi_0(z)$ is the fundamental electron (e) or hole (h) ideal QW state, $\phi_i^0(\vec{\rho})$ is a s-like one particle wavefunction. The coordinates $\vec{\rho}_3$ and $\vec{\rho}_4$ are obtained through the interchange between electrons 1 and 2 in Eq. (1). They are related to $\vec{\rho}_1$ and $\vec{\rho}_2$ through :

$$\vec{\rho}_3 = \frac{m_e}{m} \vec{\rho}_1 + \vec{\rho}_2$$

$$\vec{\rho}_4 = \left[1 - \left(\frac{m_e}{m} \right)^2 \right] \vec{\rho}_1 - \frac{m_e}{m} \vec{\rho}_2 \quad (3)$$

We limit our basis to the fundamental QW states and s-like orbitals. Although it is known that they are not sufficient for a quantitative trion description[18], the present choice retains the main physical results of the defects influence on the trion states.

Using gaussian functions, it is possible to calculate analytically all the defect potential contributions. Therefore, we chose this kind of variational wavefunction to represent the in-plane one particle state :

$$\phi_j^0(\vec{\rho}) = \frac{1}{\sqrt{2\pi}} \frac{2}{\lambda_j} \exp \left[-\frac{\rho^2}{\lambda_j^2} \right] \quad (4)$$

where λ_j is the variational parameter.

Analogously to the charged exciton case, the trial wavefunction for the neutral complex, the exciton, is given by :

$$\psi_0 = N_{i,j} \cdot \chi_0(z_h) \cdot \chi_0(z_e) \cdot \phi_i^0(\vec{R}_{ex}) \cdot \phi_j^0(\vec{\rho}) \quad (5)$$

where :

$$\begin{aligned} \vec{R}_{ex} &= \frac{m_e \vec{\rho}_e + m_h \vec{\rho}_h}{m} \\ \vec{\rho} &= \vec{\rho}_e - \vec{\rho}_h \end{aligned} \quad (6)$$

Next, we analyze the contribution of the different terms of the Hamiltonians.

A. Exciton Hamiltonian

The actual form of the interface defects is not known and it depends on the sample growth conditions. Because of this, we represent all the defects by an average one. The defect potential is assumed to have a cylindrical symmetry with gaussian shape, lateral radius D and to be centered at the z axis. Using the relative coordinate for the in-plane motion, the exciton Hamiltonian is written as :

$$H_{ex} = H(z_e) + H(z_h) + T_{xy} + V_c + V_{def}(e) + V_{def}(h), \quad (7)$$

where :

$$H(z_{e,h}) = -\frac{\hbar^2}{2m_{e,hz}} \frac{\partial^2}{\partial z_{e,h}^2} + V_{we,wh} Y\left(\frac{L}{2} - |z_{e,h}|\right), \quad (8)$$

$$T_{xy} = -\frac{\hbar^2}{2m} \left[\frac{1}{R_{ex}} \frac{\partial}{\partial R_{ex}} (R_{ex} \frac{\partial}{\partial R_{ex}}) + \frac{1}{R_{ex}^2} \frac{\partial^2}{\partial \theta_{ex}^2} \right] - \frac{\hbar^2}{2\mu} \left[\frac{1}{\rho} \frac{\partial}{\partial \rho} (\rho \frac{\partial}{\partial \rho}) + \frac{1}{\rho^2} \frac{\partial^2}{\partial \theta^2} \right], \quad (9)$$

$$V_c = -\frac{e^2}{\varepsilon \sqrt{(z_e - z_h)^2 + \rho^2}}, \quad (10)$$

$$V_{def}(e) = V_e \cdot Y\left(\frac{L}{2} < z_e < \frac{L}{2} + \delta\right) \exp \left[-\left(\frac{\vec{R}_{ex} + \frac{m_{hxy}}{m} \vec{\rho}}{D} \right)^2 \right], \quad (11)$$

$$V_{def}(h) = V_h \cdot Y\left(\frac{L}{2} < z_h < \frac{L}{2} + \delta\right) \exp \left[-\left(\frac{\vec{R}_{ex} - \frac{m_e}{m} \vec{\rho}}{D} \right)^2 \right]. \quad (12)$$

Here the QW potential height for electrons (e) and holes (h) is given by $V_{we,wh}$, $Y(z)$ is the step function ($Y(z)=1$ if $z>0$ and $Y(z)=0$ if $z<0$), L is the QW width, μ is the exciton reduced mass and ε is the GaAs dielectric constant. V_e and V_h are the QW confining potentials for electrons and holes respectively. The defect parameters are δ , the defect depth in the z direction, and D , the defect radius in the xy plane.

The X⁻ luminescence detection requires high quality samples with resolution of less than 1 meV for the excitonic photoluminescence linewidth in the case of III-V QWs. Consequently, the carriers can not be strongly localized. Therefore, we use $\delta = 1$ monolayer = 2.83 Å for GaAs and $D \sim 300$ Å [17]. Because of this, we assume that the exciton internal degrees of freedom are not strongly affected by the defect. This assumption is quantitatively estimated by the exciton energy gain due to the defect presence which should be small when compared to the energy distance between the 1S and 2S exciton levels in an ideal QW [16, 17].

B. Charged exciton Hamiltonian

Analogously to the exciton case, using the relative coordinates for the in-plane motion (Eq. (1)), the X^- Hamiltonian is given by :

$$H_{ex} = H(z_e 1) + H(z_e 2) + H(z_h) + T_{xy} + V_c + V_{def}(e1) + V_{def}(e2) + V_{def}(h) \quad (13)$$

where :

$$\begin{aligned} T_{xy} = & -\frac{\hbar^2}{2M} \left[\frac{1}{R} \frac{\partial}{\partial R} \left(R \frac{\partial}{\partial R} \right) + \frac{1}{R^2} \frac{\partial^2}{\partial \theta_R^2} \right] - \frac{\hbar^2}{2\mu} \left[\frac{1}{\rho_1} \frac{\partial}{\partial \rho_1} \left(\rho_1 \frac{\partial}{\partial \rho_1} \right) + \frac{1}{\rho_1^2} \frac{\partial^2}{\partial \theta_1^2} \right] \\ & - \frac{\hbar^2 M}{2m_e m} \left[\frac{1}{\rho_2} \frac{\partial}{\partial \rho_2} \left(\rho_2 \frac{\partial}{\partial \rho_2} \right) + \frac{1}{\rho_2^2} \frac{\partial^2}{\partial \theta_2^2} \right], \end{aligned} \quad (14)$$

$$\begin{aligned} V_c = & -\frac{e^2}{\varepsilon \sqrt{(z_{e1} - z_h)^2 + \rho_1^2}} - \frac{e^2}{\varepsilon \sqrt{(z_{e2} - z_h)^2 + |\vec{\rho}_2 + \frac{m_e}{m} \vec{\rho}_1|^2}} \\ & + \frac{e^2}{\varepsilon \sqrt{(z_{e1} - z_{e2})^2 + \left| \frac{m_{hxy}}{m} \vec{\rho}_1 - \vec{\rho}_2 \right|^2}} \end{aligned} \quad (15)$$

$$(16)$$

and the other terms follow the definition of Eq. (7). The X^+ parabolic Hamiltonian is immediately obtained through the interchange of electron and hole labels.

The charged exciton ionization energy (E_i) is defined as the difference between the energy of this charged complex and the energy of an exciton (X^0) plus an in-plane free electron (hole), in the X^- (X^+) case. Taking the ground state energy of these carriers as zero, one can write :

$$E_i(X^-/X^+) = E(X^-/X^+) - E(X^0) \quad (17)$$

It is important to realize that the charged exciton ionization energy is a difference between two values obtained through variational calculations. This means that the calculated trion ionization energy is not necessarily an upper limit of the actual value.

III. RESULTS AND DISCUSSIONS

Since we are considering a GaAs/Al_{0.3}Ga_{0.7}As QW, the effective parameters used are : $m_e=0.067m_0$, $m_{hz}=0.377m_0$, $m_{hxy}=0.112m_0$, $\varepsilon=13.2$ for the well and barrier materials. The conduction band off-set is 0.6.

We are interested in the qualitative aspects of our results. The simplicity of our trial wavefunction (Eq. (2)) does not allow us to compare the calculated ionization energies with the experimental ones. We would like to stress that the s-like functions and the fundamental QW states are not sufficient for a quantitative trion description even in the case of assuming ideal QW interfaces. However, the qualitative aspects are retained by this simple basis[18].

Figure 1 shows the X⁻ ionization energy as a function of the QW width in the cases of absence (squares) and presence (circles) of interface defects. Figure 2 shows the same calculations for the X⁺. One can see that the defect potential is more important for narrow QWs. This is a consequence of the greater amplitude of the carrier wavefunction inside the defect when narrow QWs are considered (inset of Fig. 3). Our results show that the defects play an important role and drastically affect the trion ionization energy

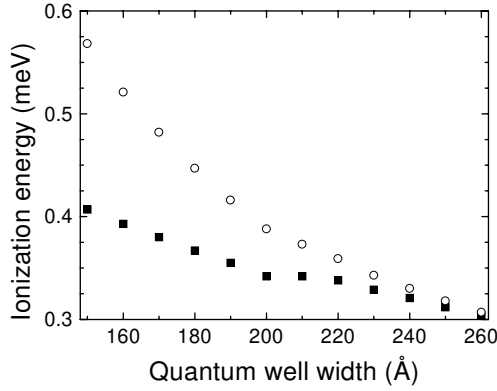


FIG. 1: X^- ionization energy as a function of a GaAs QW width in the absence (squares) and presence (open circles) of interface defects. The defect parameters are: $D = 300 \text{ \AA}$, $\delta = 1$ GaAs monolayer.

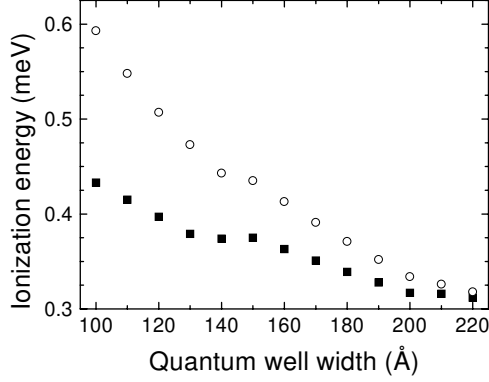


FIG. 2: *The same as Fig. 1, but for the X^+*

even in the case of a single monolayer fluctuation. They also may indicate the reason why the theoretical results have better experimental agreement in the wide QW limit[8, 18]. We show a QW width range where the trion internal degrees of freedom are not strongly affected by the defects. The criterion used was to show the points with less than 40% of energy gain due to the defect potential presence. In the wide QW limit the trion CM is almost unbound, the ionization energy tend to be that one in the ideal interface case

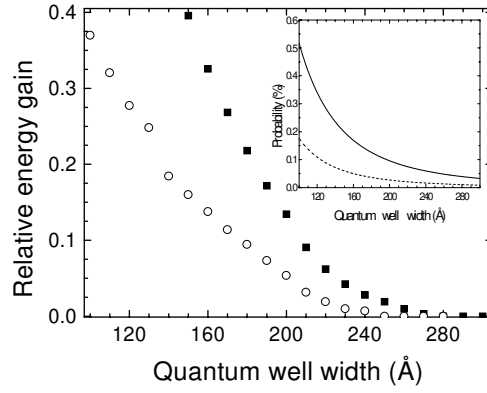


FIG. 3: X^- (squares) and X^+ (open circles) relative energy gain as a function of QW width. Inset : probability of finding an electron (solid line) or a hole (dashed line) inside the defect as a function of QW width. The defect parameters are : $D = 300 \text{ \AA}$, $\delta = 1 \text{ GaAs monolayer}$.

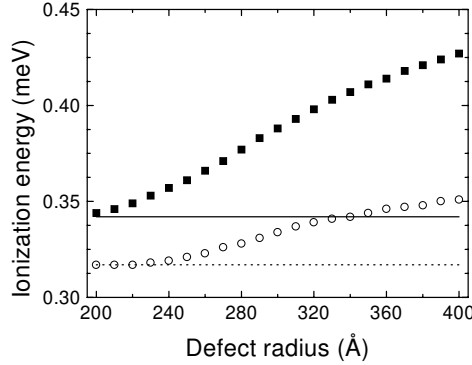


FIG. 4: X^- (squares) and X^+ (open circles) ionization energies as a function of the defect radius. The horizontal lines are the X^- (solid) and the X^+ (dotted) ionization energies in the absence of defects. The QW width is 200 Å and $\delta = 1$ GaAs monolayer.

and a gaussian function is no more able to represent such a CM state.

It is important to realize that the X^- is more strongly affected by the defect than the X^+ . This happens because the amplitude of the carrier wavefunction inside the defect is greater for electrons than for holes (inset of Fig. 3). The electron is lighter than the hole and, for the QW widths considered here, it has a greater penetration in the barrier. Consequently, electrons are more sensitive to the defect presence. In Fig. 3, we compare

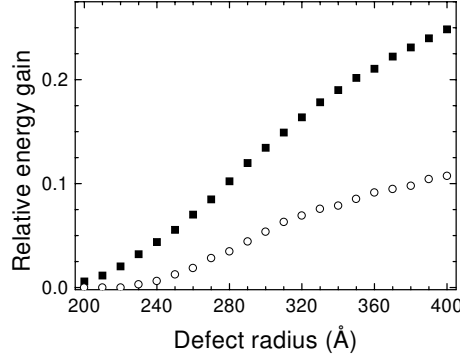


FIG. 5: X^- (squares) and X^+ (open circles) relative energy gain as a function of the defect radius. The QW width is 200 Å and $\delta = 1$ GaAs monolayer.

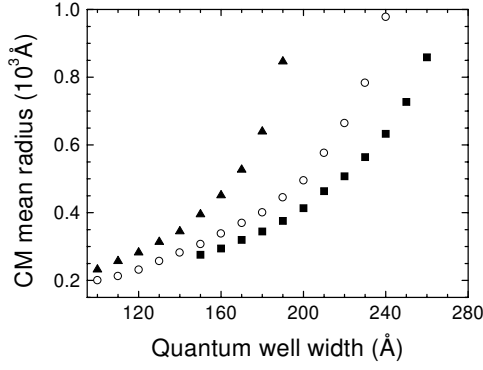


FIG. 6: *CM mean radius as a function of QW width for the exciton (up triangles), X^- (squares) and X^+ (open circles).* The defect parameters are : $D = 300 \text{ \AA}$, $\delta = 1 \text{ GaAs monolayer}$.

the X^- (squares) and the X^+ (circles) relative energy gains what means the ionization energy difference between the cases with and without defect over the last one.

Figures 4 and 5 show the defect radius influence on the trion ionization energy. The QW width is 200 Å and the defect depth is 1 GaAs monolayer. For defect radii greater than 400 Å it is expected an ionization energy saturation because, in the large defect radius limit, the system tends to be equivalent to an ideal QW but one monolayer wider. It is important to realize that, with increasing defect radius, the X^- (squares) and the

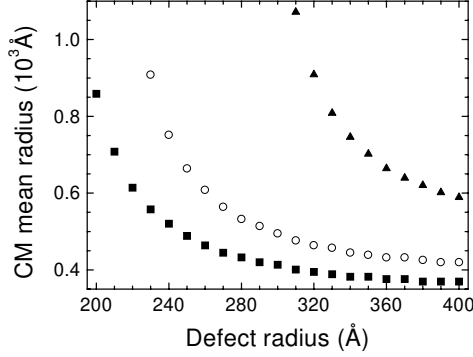


FIG. 7: *CM mean radius as a function of the defect radius for the exciton (up triangles), X^- (squares) and X^+ (open circles).* The QW width is 200 Å and $\delta = 1 \text{ GaAs monolayer}$.

X^+ (circles) ionization energies get farther and farther as a consequence of the greater electronic defect sensitivity.

Figure 6 shows the CM mean radius of exciton (triangles), X^- (squares) and X^+ (circles) as a function of the QW width. Figure 7 also shows the CM mean radii but as a function of the defect radius. One can see that the X^- is much more affected by the interface defects than the exciton, in other words, the X^- CM is more strongly localized by structural imperfections. This is in agreement with Eytan *et al.*[13]. However, they attributed the origin of this strong localization of charged complexes to fluctuations in the electrical potential of remote ionized donors. Our results show that even for strictly structural defects the X^- is more affected than the exciton.

In the limits of wide QWs and short defect radii, when the defect is less important, the CMs are weakly localized. This can be seen through the tendency to very large CM radii in Figs. 6 and 7. In these limits, the in-plane CM motion is almost unbound, consequently, it is not well represented by a gaussian function. The opposite limit cases can also be seen in the same Figs.. The X^- points in Fig. 6 are interrupted in the narrow QW region where our approximations are less adequate.

IV. CONCLUSION

We presented a simple model to take into account the interface defects contribution on the trion ionization energy. The defects are represented by a gaussian potential centered at the growth direction. Our results show that the structural imperfections are more important in the case of narrow QWs and that the charged excitons are more strongly localized than the neutral one even in the case of strictly structural defects. This explains why the theoretical results have, in general, better experimental agreement in the wide QW limit. Our results also show that the negative trion is more sensitive to the structural imperfections than the positive one.

V. ACKNOWLEDGEMENTS

This work is supported by FAPESP (Brazil) and CNPq (Brazil).

REFERENCES

- [1] M. A. Lampert, Phys. Rev. Lett. **1**, 450 (1958).
- [2] G. Munsch and B. Stébé, Phys. Status Solidi (b) **64**, 213 (1974).
- [3] B. Stébé and A. Ainane, Superlattices Microstruct. **5**, 545 (1989).
- [4] K. Kheng, R. T. Cox, Y. Merle d'Aubigné, Franck Bassani, K. Saminadayar and S. Tatarenko, Phys. Rev. Lett. **71**, 1752 (1993).
- [5] G. Finkelstein, V. Umansky, I. Bar-Joseph, V. Ciulin, S. Haacke, J.-D. Ganiere and B. Deveaud, Phys. Rev. B **58**, 12637 (1998).
- [6] C. Riva, F. M. Peeters and K. Varga, Phys. Rev. B **63**, 115302-1 (2001).
- [7] D. M. Whittaker and A. J. Shields, Phys. Rev. B **56**, 15185 (1997).
- [8] C. Riva, F. M. Peeters and K. Varga, Phys. Rev. B **61**, 13873 (2000).
- [9] S. Glasberg, G. Finkelstein, H. Shtrikman and I. Bar-Joseph, Phys. Rev. B **59**, R10425 (1999).
- [10] G. Finkelstein, H. Shtrikman, I. Bar-Joseph, Phys. Rev. B **53**, R1709 (1996).
- [11] Z. C. Yan, E. Goovaerts, C. Van Hoof, A. Bouwen, G. Borghs, Phys. Rev. B **52**, 5907 (1995).
- [12] A. J. Shields, M. Pepper, D. A. Ritchie, M. Simmons and G. A. C. Jones, Phys. Rev. B **51**, 18049 (1995).
- [13] G. Eytan, Y. Yayon, M. Rappaport, H. Shtrikman and I. Bar-Joseph, Phys. Rev. Lett. **81**, 1666 (1998).
- [14] A. B. Dzyubenko and A. Yu. Sivachenko, Phys. Rev. Lett. **84**, 4429 (2000).
- [15] V. Ciulin, P. Kossacki, S. Haacke, J.-D. Ganière, B. Deveaud, A. Esser, M. Kutrowski and T. Wojtowicz, Phys. Rev. B **62**, R16310 (2000).
- [16] G. Bastard, C. Delalande, M. H. Meynadier, P. M. Frijlink and M. Voos, Phys. Rev. B **29**, 7042 (1984).

[17] O. Heller, Ph. Lelong and G. Bastard, Phys. Rev. B **56**, 4702 (1997).

[18] L. C. O. Dacal and J. A. Brum, not published.

Capítulo 5

Negatively charged donors in semiconductor quantum wells in the presence of longitudinal magnetic and electric fields

Luis C. O. Dacal¹, José A. Brum^{1,2}

(1)IFGW-DFMC, Universidade Estadual de Campinas,

C.P. 6165, 13083-970, Campinas-SP, Brazil and

(2)Laboratório Nacional de Luz Síncrotron - ABTLuS,

C. P. 6192, 13084-971, Campinas-SP, Brazil

Abstract

We present variational calculations of the binding energy for negatively charged donors in GaAs/Al_{0.3}Ga_{0.7}As quantum wells. We show that the electronic quantum well ground state and parabolic energy dispersions are enough to obtain accurate results comparing with previous Monte Carlo calculations. The configuration interaction method is used with a physically meaningful basis set. We study the charged donor binding energy dependence on the quantum well width and donor position in the presence of external electric and magnetic fields.

I. INTRODUCTION

A negatively charged donor (D^-) is the simplest system to study many-body effects in condensed matter physics. In the case of a semiconductor quantum well (QW), its binding energy is increased by the one dimensional confinement making easier its experimental observation. Consequently, the negatively charged donor is the ideal system to improve the comprehension about exchange and correlation effects in low-dimensional structures.

A QW is a layer of low energy gap material grown between two others with larger gaps (barriers). This energy difference gives rise to electron and hole confinement in the lower gap material for type I QWs. In this type of semiconductor heterostructure, the optical transitions are dominated by Coulomb interactions. In order to obtain D^- states, the sample is intentionally modulation doped in the barriers to obtain an excess of carriers inside the QW. Additionally, it is weakly doped in the QW region. In this case, the doping is restricted to a single monolayer to avoid energy dispersion which would hamper the observation of D^- states. The excess of electrons in the QW gives rise to a state in which an extra electron is bound to the neutral donor thorough its electrical dipole. This state is analogous to the ion H^- in atomic physics. The advantage of working with semiconductor materials is that the intrinsic screening of the electrical interactions creates the possibility of getting, in laboratories, cyclotron energies of the same order of the Coulomb ones. This produces strong effects on the D^- binding energy and gives rise to rich experimental possibilities. It is possible to study a range of experimental conditions going from the limit in which the Coulomb interactions are the most important contributions to the D^- binding energy, to another one in which the cyclotron energies have this role. In the H^- case, this last experimental condition is only possible in astrophysical systems.

In recent years, the negatively charged donor has been subject of various theoretical and experimental works. Huant *et al.* [1] studied multiple quantum wells (MQWs) of GaAs selectively doped in order to form D^- centers inside the wells. They performed magneto-measurements and observed a dramatic enhancement of the donors binding en-

ergy with respect to the three dimensional case. In the QW width range of experimental interest, the D⁻ binding energy is greater for narrow QWs [2] where the carrier confinement is more effective. Dzyubenko *et al.* [3] studied the singlet and triplet transitions of D⁻ centers in QWs at high magnetic fields. They used MQWs samples which were planar doped at the QW center only and others that were also doped at the barriers. Their theoretical model considered the positive charge fixed at the QW center. They used the finite QW solutions to describe the z (growth) direction dynamics and Landau levels for the in-plane motion. Their results showed that some theoretically predicted triplet transitions are not observed in the experiment. Jiang *et al.* [4] studied the influence of the donor position inside the QW on the binding energy of D⁻ singlet states. They showed that while the on-well-center singlet state increases its binding energy with increasing magnetic field, the off-well-center one has the opposite behavior. This is a consequence of the more effective QW barrier repulsion that weakens the Coulomb attraction in the off-well-center case. The effect of an excess of electrons in the QW was also studied [5] and the authors showed that the singlet and triplet transitions are substantially blueshifted for increasing excess electron densities. They also showed that, at high magnetic fields, the many-electron system behaves like a collection of isolated two electrons ions.

On the theoretical point of view, several works used Chandrasekhar type variational wavefunctions [6–9]. Pang and Louie [10] studied on-well-center D⁻ complexes in a 100 Å QW in the presence of magnetic field. The *diffusion quantum Monte Carlo method* was used to obtain very accurate results. The *local-spin-density-functional formalism* with *self-consistent corrections* was used by Xia and Quinn [11]. Fujito *et al.* [12] studied the lifetime broadening effect on the magneto-optical absorption spectrum using a linear combination of *anisotropic gaussians* as variational wavefunctions. Marmorkos *et al.* [13] and Riva *et al.* [14] worked with effective two dimensional Coulomb interactions considering only the fundamental QW solution. The Hamiltonian was solved through the *finite difference technique*. Marmorkos *et al.* [13] studied three different configurations for a double QW situation : the D⁻ in the center of one QW, the D⁻ with one electron in

the neighbor well and the D⁻ with the two electrons in the neighbor well. They showed that the last configuration gets unbound for a magnetic field lower than 15 T, but the previous one remains bound up to 60 T. Riva *et al.* [14] studied the D⁻ binding energy as a function of magnetic field for various total angular momentum values and donor positions inside the QW. They found that singlet-triplet binding energy crossing is more probable for D⁻ complexes localized far from the well center.

In this paper, we present variational calculations of binding energy for negatively charged donors in GaAs/Al_{0.3}Ga_{0.7}As QWs. We show that a simple but physically meaningful basis set is sufficient to obtain very accurate results. The configuration interaction method with parabolic energy dispersions and only the fundamental QW state are used. We study the D⁻ binding energy dependence on the QW width and donor position in the presence of external electric and magnetic fields applied along the growth direction.

II. MODEL

We consider a GaAs QW with Al_{0.3}Ga_{0.7}As barriers treated within the effective mass and envelope function frameworks. The z axis indicates the growth direction and the position z = 0 is the QW center. We consider ideal QW interfaces, neglect the excess of carriers effects and approximate the conduction subband by a parabolic dispersion.

We start with the assumption that the QW confinement is strong enough to make a z and (x,y) separable wavefunction in the electronic basis set reasonable. We use the noninteracting electron QW ground state as the z-part of the trial wavefunction. The positive charge is the donor which is fixed inside the QW. When a longitudinal electric field (z axis) is present, the QW solution is given by the usual Airy function [15].

We label the states through the quantum numbers associated with the constants of motion, namely, the z component of the total angular momentum ($M=m_1+m_2$) and the total electronic spin ($S=S_1+S_2$). Therefore, the D⁻ states are written as singlet and triplet states.

The two electrons of D⁻ are indistinguishable and the configuration interaction method is used to build a non-orthogonal basis, in other words, we work with a basis set of Slater determinants and solve the *generalized eigenvalue problem*.

The orbital part of the D⁻ trial wavefunction with total angular momentum equal to M is given by :

$$\Psi_{(m+n=M)} = \sum_{i,j,m,n} c_{i,j,m,n} N_{i,j,m,n} \chi_0(z_{e1}) \chi_0(z_{e2}) \times [\phi_i^m(\vec{\rho}_1) \phi_j^n(\vec{\rho}_2) \pm \phi_j^n(\vec{\rho}_1) \phi_i^m(\vec{\rho}_2)], \quad (1)$$

where $c_{i,j,m,n}$ is a linear variational parameter, $N_{i,j,m,n}$ is the determinant normalization, $\chi_0(z)$ is the electronic fundamental QW state, $\phi_i^m(\vec{\rho})$ is the in-plane coordinate wavefunction. The sum over the integer numbers m and n is restricted by the conservation of the z component of the total angular momentum : $M=m+n$. In Eq. (1) “+” is for the singlet states while “-” is for the triplet ones. In the absence of magnetic field, only the singlet state with $M=0$ is a bound state.

The in-plane trial wavefunction is given by :

$$\phi_j^m(\vec{\rho}) = N_{j,m} \rho^m \exp \left[-\frac{\rho^2}{\lambda_j^2} \right] \exp [i.m.\theta] \quad (2)$$

where $N_{j,m}$ is the function normalization, m is an integer, λ_j is an element of a set of physically meaningful parameters that determines the basis size. There is one set of λ parameters for each angular momentum (m). They are chosen through a geometric progression [16].

The main advantages of the trial wavefunction (Eq. (1)) rely on its analytical integration and its physical transparency. The coordinates are composed by one positive and one negative charge, therefore, we work with in-plane functions that have the symmetry of two-dimensional atomic orbitals.

Analogously to the charged donor case, the trial wavefunction for the neutral complex is given by :

$$\psi_m = \sum_k c_k N_k \chi_0(z_e) \phi_k^m(\vec{\rho}) \quad (3)$$

In the following, we analyze the two different donor complexes.

A. Neutral Donor Hamiltonian

We describe the longitudinal magnetic field through the Coulomb gauge ($\vec{A} = \frac{1}{2}\vec{B} \times \vec{r}$) and the neutral donor Hamiltonian is written as :

$$H_{d0} = H_z + T_{xy} + V_c + V_B, \quad (4)$$

where

$$H_z = -\frac{\hbar^2}{2m_e} \frac{\partial^2}{\partial z_e^2} + V_{we} Y\left(\frac{L}{2} - |z_e|\right) + |e|Fz_e, \quad (5)$$

$$T_{xy} = -\frac{\hbar^2}{2m_e} \left[\frac{1}{\rho} \frac{\partial}{\partial \rho} \left(\rho \frac{\partial}{\partial \rho} \right) + \frac{1}{\rho^2} \frac{\partial^2}{\partial \theta^2} \right], \quad (6)$$

$$V_c = -\frac{e^2}{\varepsilon \sqrt{(z_e - z_{imp})^2 + \rho^2}}, \quad (7)$$

$$V_B = -i\hbar \frac{|e|}{c.m_e} \frac{B}{2} \frac{\partial}{\partial \theta} + \frac{e^2}{2.c^2.m_e} \frac{B^2 \cdot \rho^2}{4}. \quad (8)$$

Here, the QW potential height for the electrons is given by V_{we} , $Y(z)$ is the step function ($Y(z)=1$ if $z>0$ and $Y(z)=0$ if $z<0$), L is the QW width, F and B are the magnitude of the longitudinal electric (see Fig. 1) and magnetic fields respectively, ε is the GaAs dielectric constant and z_{imp} is the donor position.

The angular momentum conservation assumes a simple form in the neutral donor case. The ground state basis set is built up with only s-like functions. This means that m is a good quantum number and only $m=0$ terms have to be taken into account in Eq. (3). We obtain good convergence for the neutral donor ground state binding energy with 8 lambda factors between 50 and 800 Å.

B. Negatively charged donor Hamiltonian

Analogously to the neutral donor case, the D⁻ Hamiltonian is written as :

$$H_{cd} = H_{d01} + H_{d02} + V_{CR}, \quad (9)$$

where

$$V_{CR} = \frac{e^2}{\varepsilon \sqrt{|\vec{\rho}_1 - \vec{\rho}_2|^2 + (z_{e1} - z_{e2})^2}}.$$

Here, H_{d01} (H_{d02}) is the neutral donor Hamiltonian for the electron 1 (2).

The negatively charged donor binding energy (E_b) is defined as the difference between the energy of this charged complex and the energy of a neutral donor (D^0) plus an in-plane electron in the first Landau level :

$$E_b(D^-) = E(D^-) - E(D^0) - E_{LL}(e) \quad (10)$$

It is important to emphasize that the charged donor binding energy is a difference between two energies obtained variationally. This means that the calculated binding energy may not be an upper limit of the actual value. We obtain good convergence for the charged donor ground state binding energy with 8 lambda factors between 50 and 800 Å for the s-like orbitals and between 100 and 1600 Å for the p and d-like ones. This builds up a basis set with 164 states.

III. RESULTS AND DISCUSSIONS

Since we are considering a GaAs/Al_{0.3}Ga_{0.7}As QW, the effective parameters used are : $m_e=0.067m_0$ and $\varepsilon=13.2$ for the well and barrier materials. The conduction band off-set is 0.6.

The electrons indistinguishability changes the particle angular momentum conservation allowing the inclusion of nonzero angular momentum orbitals in the basis set but maintaining the total angular momentum conservation. Figure 2 shows the D^- binding energy as a function of QW width with $z_{imp}=0$ for three different levels of approximation in the basis. One can see there the importance of going beyond the s-like states approximation (solid line). This is a consequence of the Coulomb interaction between

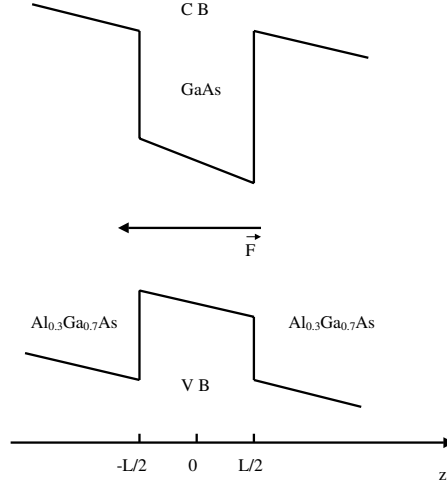


FIG. 1: *Schematic conduction and valence bands in the growth direction in the presence of longitudinal electric field.*

the electrons since the s-like orbitals favor the electrons being close while the other orbitals permit the electrons being far from each other what is imposed by the Coulomb repulsion. When the p-like states are included in the basis set (dashed line), one gets a binding energy gain of the order of 30%. This means that the s-like states are the most important ones, but they are not sufficient to reach a good binding energy convergence. The d states are relatively less important (dotted line) and we assume that a good convergence is obtained with only s, p and d orbitals in the basis. Considering all these angular momentum contributions and only the electron QW ground state we obtain an accuracy of more than 90% comparing with the D⁻ binding energy calculated by Pang and Louie [10] using *diffusion quantum Monte Carlo method*. This suggests us that the QW fundamental state approximation is a satisfactory one. Excellent agreement with Riva *et al.*[14] results is also obtained. It is better for the on-well-center donor case.

Fig. 3 shows the D⁻ binding energy as a function of the QW width for three different donor positions : $z_{imp}=0$ (solid line), $z_{imp}=L/4$ (dashed line) and $z_{imp}=L/2$ (dotted line).

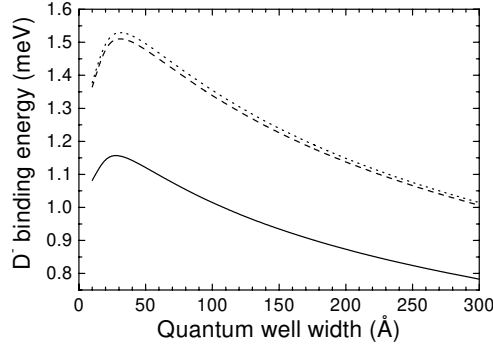


FIG. 2: D^- binding energy as a function of QW width for the on-well-center case. The results with only s -like states (solid line), s and p -like states (dashed line), s , p and d -like states (dotted line) in the basis are shown.

The results show an increase in the D^- binding energy as the QW narrows reaching a maximum of the order of 1.5 meV for $L \sim 30 \text{ \AA}$ due to the strong carrier confinement. As the donor is displaced from the QW center, the D^- binding energy decreases. This is a consequence of the barrier repulsion that prevents the electron states to be close to the attractive potential. This effect is more important for wide QWs since, in this case, the opposite barrier has less influence. As a result, the QW center is the best donor

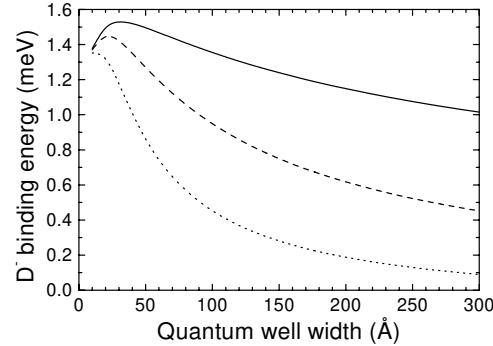


FIG. 3: D^- binding energy as a function of QW width. Three donor positions are considered : at the well center (solid line), at $L/4$ (dashed line) and at the barrier (dotted line).

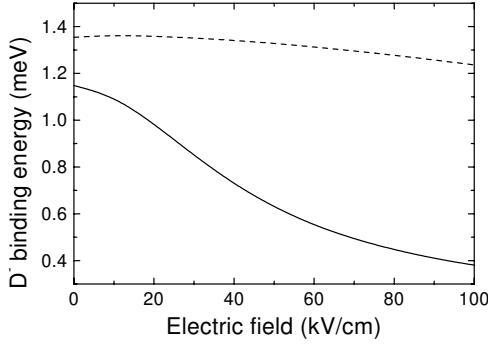


FIG. 4: D^- binding energy as a function of longitudinal electric field for $L=100 \text{ \AA}$ (dashed line) and $L=200 \text{ \AA}$ (solid line) for on-center donors.

position to observe the D^- spectrum. To resolve the D^- photoluminescence peak in the off-center cases, the lower D^- binding energies require samples with narrower neutral donor photoluminescence linewidth.

In Figure 4 we plot the D^- binding energy as a function of longitudinal electric field for $L=100 \text{ \AA}$ (dashed line) and $L=200 \text{ \AA}$ (solid line) in the case of $z_{imp}=0$. Due to the presence of a longitudinal electric field, the electrons are moved towards one of the QW

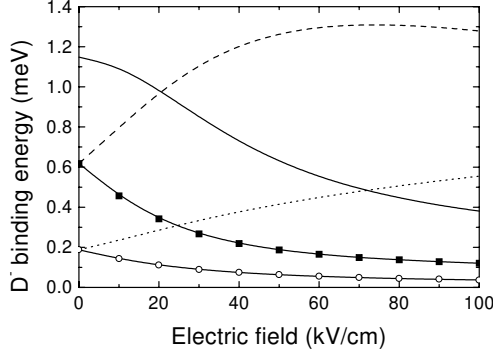


FIG. 5: D^- binding energy as a function of longitudinal electric field for $L=200 \text{ \AA}$. Several donor positions are considered : $z_{imp}=0$ (solid line), $z_{imp}=L/4$ (dashed line), $z_{imp}=-L/4$ (squares), $z_{imp}=L/2$ (dotted line), $z_{imp}=-L/2$ (open circles).

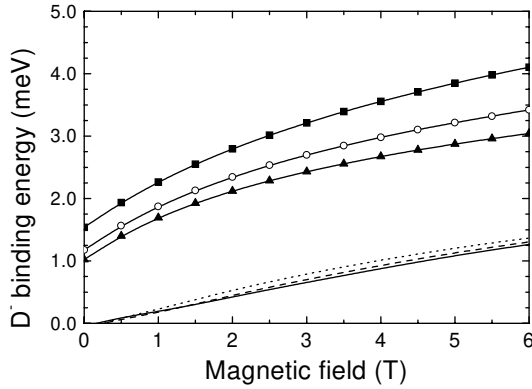


FIG. 6: D^- binding energy as a function of longitudinal magnetic field for the on-center case. Three QW widths are considered : $L=100 \text{ \AA}$ singlet (squares) and triplet (solid line) states, $L=200 \text{ \AA}$ singlet (open circles) and triplet (dashed line) states, $L=300 \text{ \AA}$ singlet (triangles) and triplet (dotted line) states. The singlet states have $M=0$ and the triplet states have $M=-1$.

interfaces, what means far from the attractive potential for the on-center donor case. This effect is smoothed by the carriers confinement inside the QW, therefore, the negatively charged donors are less sensitive to the longitudinal electric field in narrow QWs. The longitudinal electric field can increase or decrease the D^- binding energy depending on the relative position of the donor. In Fig. 5 we show the D^- binding energy as a function of the longitudinal electric field for $L=200 \text{ \AA}$ and $z_{imp}=0$, $z_{imp}=\pm L/4$ and $z_{imp}=\pm L/2$. When no electric field is present, the right and left sides of the QW are equivalent. As a consequence, the D^- binding energy is the same for equivalent positive and negative donor positions. This symmetry is broken by the electric field presence (see Fig. 1). For donors localized at the positive QW side, the longitudinal electric field enhances its binding energy. In this case, the negative carriers are pushed towards the positive charge center increasing the Coulomb attraction. In the opposite situation, the electrons are pushed far from the attractive center, what diminishes the binding energy.

When a longitudinal magnetic field is present, not only the singlet ($M=0$) state is bound but also the triplet ($M=-1$) one. The magnetic field changes the balance between

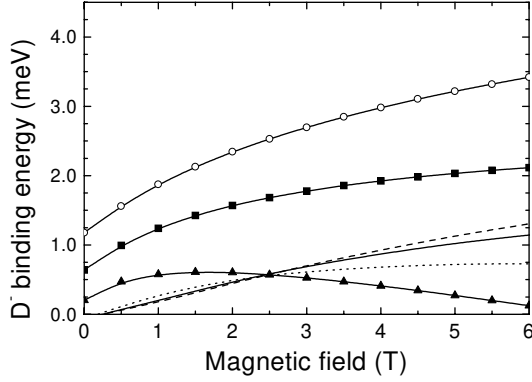


FIG. 7: D^- binding energy as a function of longitudinal magnetic field for $L=200 \text{ \AA}$. Three donor positions are considered : $z_{imp}=0$ for singlet (open circles) and triplet (dashed line) states, $z_{imp}=L/4$ for singlet (squares) and triplet (solid line) states, $z_{imp}=L/2$ for singlet (triangles) and triplet (dotted line) states.

the electron-electron repulsion and the electron-donor attraction what has different qualitative effects on the singlet and triplet states. The spatial symmetry of the triplet states leads the two particles to avoid being at the same position. On the other hand, this does not happen for singlet states (see Eq. (1)). The consequences can be seen in Fig. 6 where we show the D^- binding energy as a function of magnetic field for $L=100 \text{ \AA}$, $L=200 \text{ \AA}$ and $L=300 \text{ \AA}$ with $z_{imp}=0$. For the singlet states, the D^- binding energy decreases for wider QWs. At the same time, the opposite takes place for the triplet symmetry. However, the D^- binding energy increases with magnetic field for both types of states in the case of donors localized at the QW center. We do not foresee a triplet-singlet binding energy crossing in this situation.

Figure 7 shows the D^- binding energy as a function of the longitudinal magnetic field magnitude for our three usual donor positions in a 200 \AA QW. As one can see, for magnetic fields lower than 2.5 T, the triplet states binding energy is higher for donors at the QW interface. At the same time, the singlet states present the opposite behavior. This is a consequence of the different spatial symmetries as explained above.

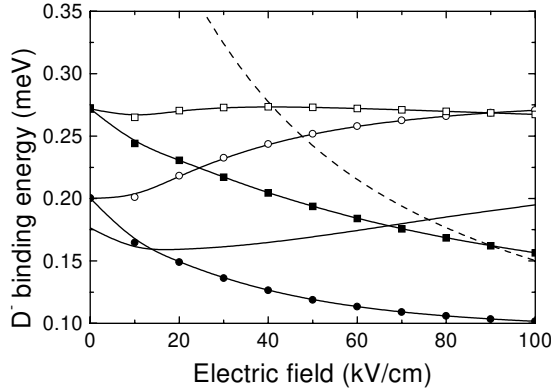


FIG. 8: D^- binding energy as a function of longitudinal electric field for $L=200$ Å in the presence of an external magnetic field of $B=1$ T. Several donor positions are considered for triplet states : $z_{imp}=0$ (solid line), $z_{imp}=-L/4$ (open circles), $z_{imp}=L/4$ (solid circles), $z_{imp}=-L/2$ (open squares), $z_{imp}=L/2$ (solid squares). Just one singlet state is shown with $z_{imp}=-L/2$ (dashed line).

For magnetic fields larger than 2.5 T, the cyclotron energy of the electrons starts to be important and the triplet states features change. It is important to notice the crossing between singlet and triplet binding energies at 2.5 T for donors localized at the interface. This crossing was also obtained by Riva *et al.* [14].

When a constant longitudinal magnetic field is applied, one can study the D^- triplet state binding energy as a function of the electric field magnitude. Fig. 8 shows the D^- binding energy as a function of longitudinal electric field for a 200 Å QW when a magnetic field of 1 T is applied along the growth direction. As one can see, the different spatial symmetries of singlet and triplet states gives rise again to opposite behaviors (compare with Fig. 5). When the electric field pushes the electrons closer to the attractive center, the binding energy is increased for the singlet state, but it decreases for the triplet one. A crossing between singlet and triplet binding energies is observed for electric fields around 40 kV/cm and $z_{imp}=-L/2$. We would like to point out that this energy crossing can only be observed when electric and magnetic fields are simultaneously considered.

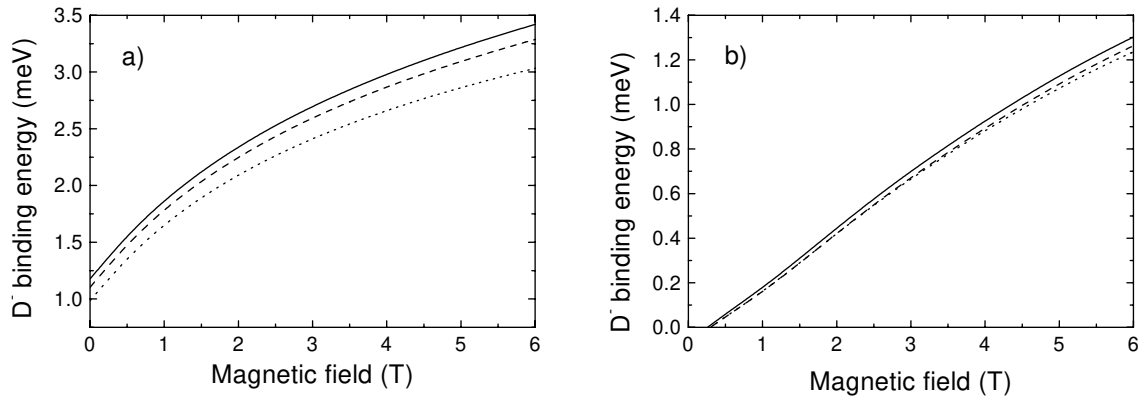


FIG. 9: D^- binding energy for the singlet $M=0$ states (a) and triplet $M=-1$ states (b) as a function of longitudinal magnetic field for $L=200$ Å and donors localized at the QW center. Three longitudinal electric fields values are considered : $F=0$ kV/cm (solid line), $F=10$ kV/cm (dashed line) and $F=20$ kV/cm (dotted line).

Figure 9 presents the D^- binding energy as a function of longitudinal magnetic field in the case of on-center donors and $L=200$ Å for three values of longitudinal electric fields : 0 kV/cm (solid line), 10 kV/cm (dashed line) and 20 kV/cm (dotted line). One can see that the presence of a longitudinal electric field does not change the qualitative aspects of the D^- binding energy behavior as a function of magnetic field. What can also be seen is that the singlet states are more sensitive to the electric field presence than the triplet ones.

Finally, in Fig. 10, we compare our results with the experimental data from Huant *et al.* [1] (squares) obtaining a good qualitative agreement. An important source of inaccuracies may be the electrons localization by the QW interface roughnesses which increases the D^- binding energy. We also show a comparison with the theoretical results of Pang and Louie[10] (star). We would like to point out that we obtain an excellent agreement with the more sophisticated *diffusion quantum Monte Carlo method* used by them . This confirms the quality of our simple D^- description.

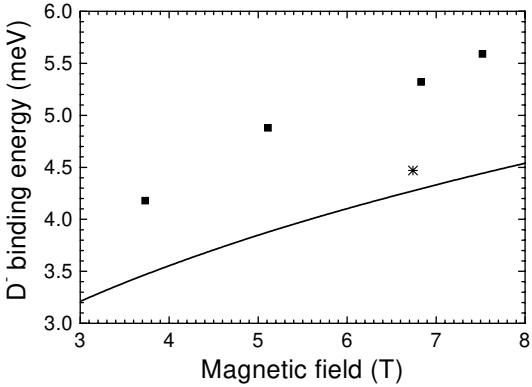


FIG. 10: D^- binding energy as a function of longitudinal magnetic field for $L=100 \text{ \AA}$ and donors localized at the QW center. The squares are experimental data from Huant et al.[1], the star is the value obtained by Pang and Louie[10] and the solid line corresponds to our results.

IV. CONCLUSION

In conclusion, we variationally calculated the D^- binding energy in GaAs/Al_{0.3}Ga_{0.7}As semiconductor QWs. The effects of longitudinal electric and magnetic fields were studied for several donor positions inside the QW. We showed that the crossing of the binding energies of singlet and triplet states can be controlled through the donor position inside the QW and through the application of external fields.

Our results show a very good agreement with *diffusion quantum Monte Carlo method* results[10]. This proves that our approach retains the most important physical characteristics of the studied complexes. We believe that the effects of carriers localization due to the QW interface roughnesses are the main sources of the discrepancies between the experimental binding energies and ours.

V. ACKNOWLEDGEMENTS

This work is supported by FAPESP (Brazil) and CNPq (Brazil).

REFERENCES

- [1] S. Huant, S. P. Najda and B. Etienne, Phys. Rev. Lett. **65**, 1486 (1990).
- [2] S. Huant, A. Mandray, J. Zhu, S. Louie, T. Pang and B. Etienne, Phys. Rev. B **48**, 2370 (1993).
- [3] A. Dzyubenko, A. Mandray, S. Huant, A. Sivachenko and B. Etienne, Phys. Rev. B **50**, 4687 (1994).
- [4] Z. Jiang, B. McCombe, J. Zhu and W. Schaff, Phys. Rev. B **56**, R1692 (1997).
- [5] Z. Jiang, B. McCombe and P. Hawrylak, Phys. Rev. Lett. **81**, 3499 (1998).
- [6] D. Larsen and S. McCann, Phys. Rev. B **46**, 3966 (1992).
- [7] N. Sandler and C. Proetto, Phys. Rev. B **46**, 7707 (1992).
- [8] J. Zhu and S. Xu, Phys. Rev. B **50**, 12175 (1994).
- [9] J. Zhu, D. Lin and Y. Kawazoe, Phys. Rev. B **54**, 16786 (1996).
- [10] T. Pang and S. Louie, Phys. Rev. Lett. **65**, 1635 (1990).
- [11] X. Xia and J. Quinn, Phys. Rev. B **46**, 12530 (1992).
- [12] M. Fujito, A. Natori and H. Yasunaga, Phys. Rev. B **51**, 4637 (1995).
- [13] I. Marmorkos, V. Schweigert and F. Peeters, Phys. Rev. B **55**, 5065 (1997).
- [14] C. Riva, V. Schweigert and F. Peeters, Phys. Rev. B **57**, 15392 (1998).
- [15] J. A. Brum, C. Priester, and G. Allan, Phys. Rev. B **32**, 2378 (1985).
- [16] C. Aldrich and R. L. Greene, Phys. Status Solidi (b) **93**, 343 (1979).

Capítulo 6

Conclusão geral

O exciton negativamente carregado (X^-) e o doador negativamente carregado (D^-) constituem os sistemas mais simples para estudo dos efeitos de correlação e troca em física de semicondutores. No caso do estudo destes complexos em poços quânticos, o confinamento unidimensional das cargas e consequente discretização de suas dinâmicas aumenta enormemente a energia de ligação destes complexos.

Nosso trabalho mostrou que, na ausência de campos magnéticos, apenas o estado singlet com a componente z do momento angular total de partícula relativa igual a zero ($M=0$) é ligado. A presença de campo magnético longitudinal liga também o estado triplex com $M=-1$. Isto ocorre tanto para o X^- quanto para o D^- .

A diferença na simetria espacial entre as funções tipo singlet e triplex é um fator determinante no comportamento da energia de ligação do complexo em função da largura do poço. No caso do doador negativamente carregado e fixo fora do centro do poço, esta simetria espacial também influencia fortemente o comportamento da energia de ligação em função do valor do campo elétrico longitudinal. Mostramos ainda que, de maneira geral, os estados triplex são menos sensíveis à ação destes campos elétricos.

A necessidade da utilização de uma base flexível para uma boa representação do X^- ficou clara. Nossos resultados mostraram que é essencial ir além da aproximação de estado fundamental de poço para elétrons. Este efeito está ligado à indistinguibilidade destas cargas uma vez que ele não se verifica no caso do exciton. Outro exemplo importante é a necessidade da inclusão de mais de um nível de Landau para o centro de massa quando da presença de campo magnético. É importante ressaltar que, no caso do doador negativamente carregado, considerar apenas o estado fundamental dos elétrons no poço nos leva a obter excelentes resultados. Isto mostra que a ausência de mobilidade do centro atrativo (carga positiva) altera fortemente a física do complexo.

As dúvidas atualmente presentes dizem respeito ao caráter livre ou localizado das cargas que formam o X^- . Isto nos levou a analisar os efeitos da presença de defeitos estruturais na interface entre poço e barreira. Nós mostramos que os “trions” são mais

fortemente afetados pela presença destes defeitos que o exciton. Estes defeitos sempre se formam durante o processo de crescimento da heteroestrutura e desempenham um papel importante na dinâmica dos “trions”. Isto é atestado pela resposta óptica do estado fundamental tipo tripleno, o qual só é opticamente ativo devido à quebra de simetria translacional induzida, provavelmente, pela presença destes defeitos estruturais.

Tudo isto nos permite afirmar que a principal causa da discordância entre nossos resultados e os obtidos experimentalmente é a não inclusão dos efeitos destes defeitos estruturais nos nossos cálculos com uma base suficientemente flexibilizada.

Uma conclusão definitiva a respeito da existência e natureza dos potenciais que localizam as cargas do “trion” necessita de mais análises experimentais e merece um modelamento teórico mais flexível que aquele que nós utilizamos para este caso.

Outra perspectiva interessante para estudo do “trion” diz respeito a seus processos de formação e recombinação. A presença do excesso de portadores no poço e a influência deste na dinâmica do complexo cria um sistema “rico em física” a ser testado e compreendido.

O tratamento teórico dos “trions” fora da aproximação de dispersões parabólicas também merece atenção, pois isto deve proporcionar um certo ganho no valor calculado para a energia de ligação. Ressaltamos porém que com a introdução de um campo magnético longitudinal o Hamiltoniano não parabólico do X^- e do X^+ exigem um tratamento bastante complexo e os resultados experimentais atualmente disponíveis não permitem uma resolução suficiente para a observação de possíveis efeitos decorrentes da não parabolicidade das bandas.